

Marquette University

e-Publications@Marquette

Master's Theses (2009 -)

Dissertations, Theses, and Professional
Projects

An Investigation of the Effect of Trunk Musculature on the Lumbar Spine Injury During a High-Speed Frontal Central Crash

Nan Lin

Marquette University

Follow this and additional works at: https://epublications.marquette.edu/theses_open



Part of the [Engineering Commons](#)

Recommended Citation

Lin, Nan, "An Investigation of the Effect of Trunk Musculature on the Lumbar Spine Injury During a High-Speed Frontal Central Crash" (2020). *Master's Theses (2009 -)*. 628.

https://epublications.marquette.edu/theses_open/628

AN INVESTIGATION OF THE EFFECT OF TRUNK MUSCULATURE
ON THE LUMBAR SPINE INJURY
DURING A HIGH-SPEED
FRONTAL CENTRAL
CRASH

by

Nan Lin, B.E.

A Thesis submitted to the Faculty of the Graduate School, Marquette University, in Partial
Fulfillment of the Requirements for the Degree of Master of Science

Milwaukee, Wisconsin
December 2020

ABSTRACT
AN INVESTIGATION OF THE EFFECT OF TRUNK MUSCULATURE
ON THE LUMBAR SPINE INJURY
DURING A HIGH-SPEED
FRONTAL CENTRAL
CRASH

Nan Lin, B.E.

Marquette University, 2020

Motor vehicle crashes have been a leading cause of fatalities and injuries worldwide. Owing to new protection systems, the occurrence of injuries has been decreasing in recent years. On the contrary, the incidence of lumbar spine injuries in frontal crashes has been increasing as a function of the vehicle model year. However, only a few studies focused on lumbar spine injuries in vehicle crashes. Therefore, the mechanism of lumbar spine injuries has not been understood thoroughly. Muscle contraction is one of the factors that influence the risk of lumbar spine injuries as occupants tend to brace their muscles during a vehicle crash. Greater muscle contraction, especially anticipatory muscle contraction, may contribute to bony injury. This study aimed to investigate the effect of lumbar muscle activation and the timing of muscle activation on the lumbar spine injury risk during a high-speed frontal central crash by utilizing a finite element human body model. The study implemented lumbar musculature on two versions of the validated models against the experimental results from a previous study. Sixteen simulations with 8 of each version were set up. These 8 simulations included: fully activated at 0ms, 40ms, and 80ms; half activated at 0ms, 40ms, and 80ms; no activation and no muscle. The model was seated in a simplified vehicle seat extracted from a common vehicle model and was in a frontal pole/tree (central) crash scenario with an initial speed of 56km/h. Each simulation ran for 150ms and forces on vertebrae L1, L3 and L5 were collected. The results showed the lumbar spine forces increased with the muscle activation level and decreased with the timing of the muscle activation. This suggested that the anticipatory powerfully braced lumbar muscles had a higher risk to induce lumbar spine injuries. Since it is impossible to train occupants to avoid bracing in anticipation of a frontal crash, this study focuses the attention on enhanced protection for the lumbar region of vehicle occupants in the future.

ACKNOWLEDGEMENTS

Nan Lin, B.E.

I would like to express my deep appreciation to my committee members. Firstly, thank you Dr. Frank Pintar, my thesis advisor, for his advices on my thesis and his encouragement when I lost confidence. I am also extremely grateful to Dr. Sagar Umale, my laboratory mentor, for his meticulously step-by-step guidance of carrying out my research and experiments, and his kindness and patience whenever I encountered any problems. I am thoroughly grateful for Dr. Gerald Harris, especially for his patience and meaningful suggestions for my thesis.

I would also like to acknowledge the assistance and support of Mr. Prashant Khandelwal, and the many faculties at the Department of Biomedical Engineering of Marquette University as well as Neuroscience Research Lab under the Medical College of Wisconsin for their support through the whole process of my research.

Special thanks to my dear friend, Ms. Danni, and a couple of other very close friends for embracing me with warm encouragement despite of my dark times.

Finally, I would like to express my deepest gratitude to my parents, my cousin, my aunt, and all my other family members for their unwavering understanding and tremendous support which tided me over the many obstacles during my Master of Science journey.

TABLE OF CONTENTS

ACKNOWLEDGEMENT	i
LIST OF TABLES	v
LIST OF FIGURES	vi
CHAPTER	
I. INTRODUCTION	1
II. BACKGROUND.....	4
2.1 Incidence of Lumbar Spine Injuries in MVCs	4
2.2 Frontal Crash and Central Frontal Crash	6
III. LITERATURE REVIEW	9
3.1 Introduction of Volunteers and Human Surrogates Utilized in Vehicle Crash Studies	9
3.2 Experimental Studies of Lumbar Spine Compressive Tolerance	10
3.3 Human Studies on the Effect of Musculature	11
3.4 Development of HBM.....	14
3.5 HBM Studies on Effects of Muscle Contraction	20
3.6 Studies on the Effects of Crash Pulse	22
IV. FUNCTIONAL ANATOMY	25
4.1 Bony Vertebrae	25
4.2 Endplates.....	27
4.3 Facet Joints.....	27
4.4 Intervertebral Discs	28
4.5 Ligaments.....	29

4.6 Muscles	31
4.6.1 Multifidus.....	32
4.6.2 Erector Spinae.....	32
4.6.3 Quadratus Lumborum	33
4.6.4 Rectus Abdominis.....	34
4.6.5 External and Internal Oblique Muscles.....	35
4.6.6 Psoas Major.....	35
V. METHODS	37
5.1 Hill-type Muscle Model.....	37
5.2 Implementation of the Musculature	39
5.3 Validation.....	42
5.4 Investigation of the Effect of the Musculature in the High-speed Frontal Crash.....	49
VI. RESULTS	54
6.1 Validation.....	54
6.2 Results of the High-speed Frontal Crash	59
VII. DISCUSSION	67
7.1 Validation.....	67
7.2 Investigation of the Effect of the Musculature in the High-speed Frontal Crash	70
VIII. CONCLUSION	77
IX. LIMITATIONS AND FUTURE DIRECTION.....	78
BIBLIOGRAPHY	80

APPENDIX.....87

LIST OF TABLES

Table 5-2-1: Parameters of the Hill-type muscle model in this study	41
Table 5-4-1: Test matrix	50
Table 6-1-1: Peak displacement along x and z axis between HBM and 2 subjects in Ejima et al (2007)	58
Table 6-2-1: Peak compressive lumbar force (kN)	65
Table 6-2-2: Timing of peak compressive force (ms)	65
Appendix Table 1: Function, muscle layer classification, origin, insertion, PCSA, length and activation level curve used of each trunk muscle element implemented in this study....	87

LIST OF FIGURES

Figure 2-2-1 a: Between-rail crash (Morgan et al., 2012).....	7
Figure 2-2-1 b: small overlap central crash (4) (Adolph and Ott, 2015).....	7
Figure 2-2-1 c: Typical figure and code of central crash defined by NASS-CDC (Pintar et al., 2008)	7
Figure 3-4-1 a: The model of Huang et al. (1994).....	16
Figure 3-4-1 b: The model of Lizee et al. (1998)	16
Figure 3-4-2: The history of the development of the GHBM HBM (Combest, 2016).....	18
Figure 3-4-3: The Model of the GHBM HBM detailed M50	20
Figure 4-1-1: Lumbar spine and sacrum.....	26
Figure 4-1-2: Lumbar vertebra.....	26
Figure 4-3-1: Facet joints	27
Figure 4-3-2: Components of the facet joint.....	28
Figure 4-4-1: Intervertebral discs and endplates.....	29
Figure 4-5-1: Spinal ligaments.....	30
Figure 4-6-1-1: Multifidus	32
Figure 4-6-2-1: Erector spinae	33
Figure 4-6-3-1: Quadratus lumborum.....	34
Figure 4-6-4-1: Rectus abdominis	34
Figure 4-6-5-1: External and internal oblique muscles	35
Figure 4-6-6-1: Psoas major.....	36
Figure 5-1-1: A classic Hill-type muscle model (Adopted from LS-DYNA Manual	

Volume 2).....	37
Figure 5-1-2: Force-length and force-velocity curves (adopted from LS-DYNA Manual Volume 2).....	39
Figure 5-2-1: Trunk extensors: a) Erector spinae iliocostalis lumborum pars thoracis....	41
Figure 5-2-1: Trunk extensors: b) Erector spinae iliocostalis lumborum-pars lumborum	41
Figure 5-2-1: Trunk extensors: c) Erector spinae longissimus thoracis pars lumborum ..	41
Figure 5-2-1: Trunk extensors: d) Erector spinae longissimus thoracis pars thoracis.....	41
Figure 5-2-1: Trunk extensors: e) Multifidus lumborum.....	41
Figure 5-2-1: Trunk extensors: f) Multifidus thoracis	41
Figure 5-2-1: Trunk flexors: g) Quadratus lumborum muscles.....	41
Figure 5-2-1: Trunk flexors: h) rectus abdominus.....	41
Figure 5-2-1: Trunk flexors: i) External oblique muscles	41
Figure 5-2-1: Trunk flexors: j) Internal oblique muscles	42
Figure 5-2-1: Lower extremities muscle: k) Psoas major.....	42
Figure 5-3-1: Deceleration pulse (Ejima et al., 2007)	43
Figure 5-3-2: Sled test from Ejima et al. (2007).....	47
Figure 5-3-3: Setup of the validation	48
Figure 5-4-1: Activation level curves used in high-speed frontal crash simulations: a) Fully activated at 0ms	50
Figure 5-4-1: Activation level curves used in high-speed frontal crash simulations: b) Half activated at 0ms	50
Figure 5-4-1: Activation level curves used in high-speed frontal crash simulations: c) Fully activated at 40ms	51
Figure 5-4-1: Activation level curves used in high-speed frontal crash simulations: d) Half activated at 40ms	51
Figure 5-4-1: Activation level curves used in high-speed frontal crash simulations: e)	

Fully activated at 80ms	51
Figure 5-4-1: Activation level curves used in high-speed frontal crash simulations: f) Half activated at 80ms	51
Figure 5-4-1: Activation level curves used in high-speed frontal crash simulations: g) No activation.....	51
Figure 5-4-2: Acceleration pulse (Marzougui et al., 2013).....	52
Figure 5-4-3: Outlook of the seated GHBMC HBM M50 in the vehicle	53
Figure 6-1-1: Results of the validation (V4.5).....	57
Figure 6-1-2: Results of the validation (V5.0).....	58
Figure 6-2-1: Peak compressive lumbar forces (kN).....	62
Figure 6-2-2: An example of force trace: V5.0 on L3	63
Figure 6-2-3: Timing of peak compressive force (ms)	64
Figure 6-2-4: Lumbosacral spine geometry for the without muscle case at 100ms	64
Figure 7-2-1: The relationship of the risk of the injury and the lumbar spine force (Adapted from Stemper et al., 2018)	75

I. INTRODUCTION

Motor vehicle crash (MVC) injuries are a leading cause of morbidities and mortalities worldwide. Each year, more than 1.2 million people die because of the MVC injuries and millions more sustain severe injuries and live with chronic health consequences globally. Moreover, MVC are the major cause of death especially among young people between ages 15 to 29. In 2012, over 300,000 young people died because of MVCs, followed by suicide, which claimed about 250,000 livings (World Health Organization (WHO), 2015). In the United States, there were 5,687,000 police-reported MVCs which resulted in 32,719 deaths and 2,313,000 people injured (NHTSA, 2013). In the European Union, 31,506 fatalities were reported in 2010 due to MVCs (European Commission, 2017).

Spine injuries are one of the three most frequent type of injuries of MVCs (Jakobsson et al., 2016). MVCs are the second leading cause of spine injuries, following accidental falls (Pedram et al., 2010). These types of injuries may not directly result in fatality as oppose to head injuries, but they are a leading cause of disability, especially when combined with spinal cord injuries. It also contributes to high health care cost and has the lowest return-to-work rate among injuries of all major body regions. Severe compressive fractures can also cause height loss. (Pedram et al., 2010; Kaufman et al., 2013; Rao et al., 2017). The most frequent locations of spinal injuries during MVCs are the cervical and the lumbar spine. Muller et al. (2014) investigated data of front-seat occupant injuries of all body regions in Germany (year: 1988-2011). Over the study period, 280 occupants sustained vertebral injuries, where 126 had cervical injuries, 99

had lumbar injuries and 78 had thoracic injuries. Adolph et al., (2013), which studied data from the German In-Depth Accident Study (GIDAS) (car's first year of registration: 2000-2011), determined the same distribution. More specifically, C1 and C7 in the cervical region and L1 in the lumbar region had a higher risk of injuries (Adolph et al., 2013).

Although both cervical and lumbar spine have a high risk of injuries, the lumbar spine injury is unique. Fatalities and injuries resulting from MVCs have ceased to increase in recent years. The WHO reported in 2015 that the fatalities of MVCs have been plateauing globally since 2007 (WHO, 2015). In the United States, the total deaths from MVC was 36,560 in 2018, which was less than 37,473 in 2017 and much less than 44,525 in 1975. It was also found by the National Highway Traffic Safety Administration (NHTSA) that the newer model-year vehicles have a lower injury rate (Liu et al., 2020). All thanks to the usage of protective equipment such as 3-point seatbelts and airbags (Wang et al., 2009). However, some recent literature determined that the occurrence rate of lumbar spine injuries has increased as a function of the vehicle model year. In other words, occupants of newer model year vehicle had a higher risk of lumbar spine injuries. This is opposite to injuries of other body regions (Pintar et al., 2012; Kaufman et al., 2013).

As apparent from above, lumbar spine injuries are common among spinal injuries, and the risk of lumbar spine injuries has increased with occupants of newer model year vehicles as opposite to injuries of other body regions. Therefore, this study will focus on

the lumbar spinal injuries during MVCs to better understand the biomechanical mechanism so as to aid in occupant protection.

II. BACKGROUND

Motor vehicle crashes are one of the leading reasons for mortality in the US. In recent years, the rate of fatality and severe injuries in the MVC have decreased owing to the usage of 3-point seatbelts and airbags (NHTSA, 2017; Wang et al., 2009). However, it was determined from some recent literature that the incidence of lumbar spine fractures has actually increased with newer model year vehicles.

2.1 Incidence of Lumbar Spine Injuries in MVCs

Wang et al. (2009) investigated 29,860 cases of MVC from the Crash Outcome Data Evaluation System (CODES) of Wisconsin (year: 1994-2002). It was found that the occurrence of spinal fractures increased during that period corresponding to an increase usage of seatbelts and airbags, but the occurrence of severe lumbar spine fractures (Abbreviated Injury Scale Score (AIS) 3+) has not increased significantly.

Doud et al. (2015) also observed an increase of lumbar spine injuries (from 19,836 to 29,428) from the investigation of the National Inpatient Sample (NIS) database (year: 1998 to 2007). Additional investigation of the National Trauma Database (NTDB) (year: 2002-2006) showed that the number of AIS2+ thoracolumbar injuries increased from 7,058 to 11,391.

A more specific trend demonstrated that thoracolumbar spine fractures only increased in frontal crashes. Pintar et al. (2012) investigated the National Automotive Sampling System (NASS) – Crashworthiness Data System (CDS) database (year: 1986-2008) and Crash Injury Research and Engineering Network (CIREN) database. It

was observed that the occurrence of thoracolumbar fractures increased as a function of the vehicle model year in the frontal crash. The vehicle model year in the US is defined as the year the vehicle is manufactured. A year cycle is usually from the October of the last year to the September of the current year. However, this trend did not occur in other types of crashes. It was also observed that each year, 2,000-4,000 occupants sustained thoracolumbar spine fractures in a frontal crash. The number was always higher than for other types of crashes. The lower thoracic (T10-T12) and lumbar spine had a higher occurrence of fractures. L1 was the most frequently injured location (Pintar et al., 2012).

Similar results were also observed by Kaufman et al. (2013). Data from the NASS (year: 1993-2011) showed that the percentage of cases involving major compression lumbar spine fractures in direct frontal crashes was higher in the later model year. This percentage was 2.5 and 2 times greater in model years later than 2000 compared to the 1990s and 1980s, respectively. From the CIREN database (year: 1996-2012), it was also found that most of the major compression lumbar spine fractures in frontal crashes were with vehicle model years later than 2004 (Kaufman et al., 2013).

These studies not only confirm that the occurrence of lumbar spine fracture has increased in frontal crashes, but also confirmed that the most frequent crash resulting in lumbar spine fracture is the frontal crash. Jakobsson et al. (2016) investigated the data of crash occupants in vehicles of model years from 1999-2013 from the Volvo Cars Traffic Accident Database. It was also observed that the spine was one of the top three body regions sustaining injuries, and thoracolumbar injuries were the most frequent spine

injuries. Among all reported AIS2+ thoracolumbar injuries, the frontal crash was the most common reason (36%). And 58% of all these injuries were lumbar spine injuries.

The lumbar spine fracture is a common type of injuries in MVC. This injury may not directly lead to fatality, but it can lead to morbidity, especially when associated with neurologic deficit and deformity (Rao et al., 2017). However, in the past, researchers focused more on cervical spine injuries. Forman et al. (2015) reviewed research on automobile collision impact from 1990 to 2009. It was observed that 59% of spine studies were about cervical spine injuries. Only 8% focused on thoracic and lumbar spine injuries. Therefore, the investigation of lumbar spine fracture in the frontal crash with vehicles of newer model year seems necessary.

2.2 Frontal Crash and Central Frontal Crash

The frontal crash is the most common type of crash resulting in fatality. In 2018, frontal crashes accounted for 56% of the total deaths in vehicle crashes (IIHS, n.d.). Referring to the face of a clock where 12 o'clock is the direction of forward movement, the frontal vehicle crash refers to a type of vehicle crash with major damage to a vehicle at 10, 11, 12, 1 or 2 clock position (Zador and Coccone, 1993). In polar coordinates, it is a vehicle crash in which the initial direction of the force is between -30° to $+30^{\circ}$ (Richard et al., 2006).

There are several ways to further classify frontal crashes, such as by the location of damage and the type of objects the vehicle hit. The central crash (the front center of a vehicle impact into a pole or tree) is one of them. By the location of damage, the central pole crash can be categorized into between-rail (because the damage is between two

frontal longitudinal rails of the vehicle) crash or the small/narrow overlap center crash (To make it simple, this location-defined type of crash will be called as the central crash).

The name of the category depends on the choice of crash configurations. Below are names of this type of crash from different configurations:

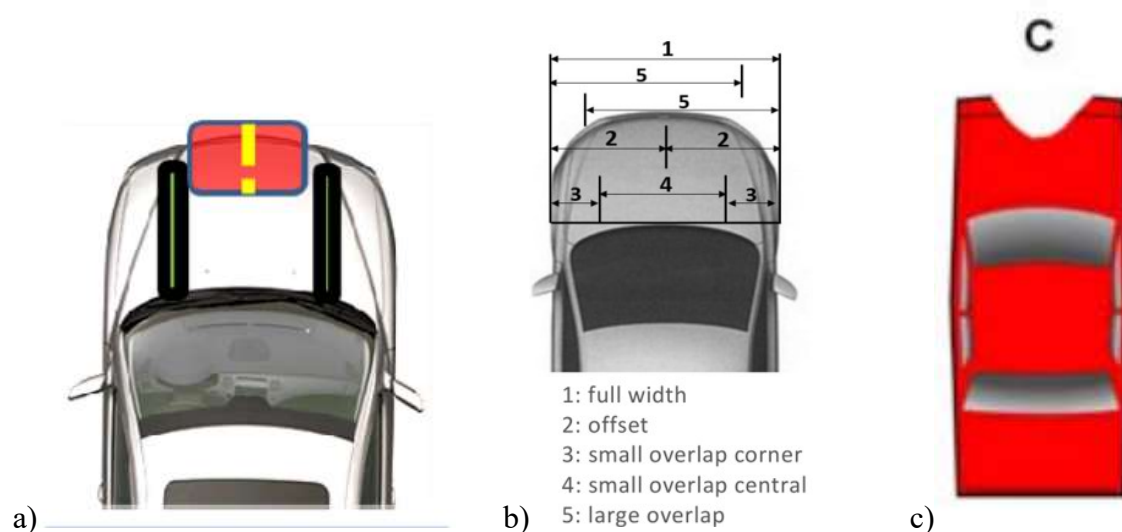


Figure 2-2-1: a) Between-rail crash (Morgan et al., 2012); **b)** small overlap central crash (4) (Adolph and Ott, 2015); **c)** Typical figure and code of central crash defined by NASS-CDC (Pintar et al., 2008)

One of the reasons that makes the central crash unique was that although the driver death rate in the frontal crash had dropped steadily, the rate of the narrow objects crashes dropped more slowly than other crashes combined (Arbelaez et al., 2006). Scullion et al. (2010) further observed that the central crash was more likely to result in injuries. They investigated 12,854 vehicles (model year: 1997-2009) from NASS-CDS. It was shown that although the central/between-rails impacts accounted for only 6.1% of the total frontal crash, the occurrence of MAIS 2+ and MAIS 3+ injuries were highest in the central impact (13.4% and 3.1%, respectively) than for other types of frontal crashes.

It was reported that, except for upper and lower extremities injuries, thoracolumbar spinal injuries were also common in central crashes (Scullion et al., 2010). It was also observed by Pintar et al. (2012) that over half of the surveyed lumbar spine fractures occurred in frontal pole impacts (17 of 30).

In conclusion, although the fatality rate of the MVC has decreased in recent years, the occurrence of the lumbar spine fracture in the frontal crash is still increasing, especially with newer model year vehicles. The lumbar spine fracture occurs more frequently in a frontal crash. Frontal crashes had the highest risk of injuries and the central crash is the most severe crash among all frontal crashes. The lumbar spine has a high risk of injuries in frontal central crashes. Moreover, there were only a few studies focused on lumbar spine injuries in the past. Therefore, a study focusing on lumbar spine fracture in a central frontal crash scenario of the newer model year vehicle may aid occupant safety.

III. LITERATURE REVIEW

This chapter will review the literature used for the current study, which lead to the key questions of the study. It will briefly introduce volunteer tests and human surrogates used in vehicle studies and the contributions of these techniques including the tolerance of lumbar spine and the effects of musculature on the risk of injuries during vehicle crashes. Then there is a focus on the Human Body Model (HBM) studies including the development of HBM with an emphasis on the Global Human Body Model Consortium (GHBMC) HBM, and the influence of muscle contraction on kinematic and kinetic responses of human observed from the HBM studies. Finally, this chapter will also focus on the severity and effect of human injuries in frontal central crash, which will explain why the current choice of acceleration pulse was used.

3.1 Introduction of Volunteers and Human Surrogates Utilized in Vehicle Crash Studies

The volunteer sled test is one of the ways to predict responses of occupants during an MVC because all the results are collected from the living human. The test usually constrains volunteers on a seat which is mounted on a ramp. The impact of the sled and damper at the end of the ramp simulates the vehicle impact deceleration pulse. Surface markers are attached to the skin of the volunteer to capture kinematic responses by cameras. Therefore, occupant responses during a low-speed MVC can be predicted by the results from the test (Ejima et al., 2007).

However, due to ethical concerns, the volunteer can only be utilized in low-speed tests, and markers can only be attached to the skin. Therefore, human cadavers and ATD

or “dummies” have been used as human surrogates to study injurious MVC scenarios. A cadaver test can also be used to predict the risk of injuries such as fractures. This is obviously not feasible in a living human volunteer. Since Lawrence Patrick in 1930 first sent a cadaver down an elevator shaft to investigate the response of the human body under high impact, the cadaver has been used widely in studies of MVC (Marqius, 2013).

An ATD, on the other hand, is also a human surrogate. A decade after the first use of the cadaver in MVC studies, the first ATD was used in the air force in 1949. After many years of development, dummies have been widely used in car crash tests (Xu et al., 2018). The results of kinematic responses of cadavers can be further used to enhance and design the response of the ATD.

in recent decades, finite element Human Body Models (HBM) have also been used as virtual surrogates to simulate vehicle crashes in software such as the LS-DYNA. The development and contributions of HBM will be introduced in the section 3.4 and 3.5.

3.2 Experimental Studies of Lumbar Spine Compressive Tolerance

Lumbar spine tolerance is the force needed to fracture the lumbar spine. It is one of the parameters that determine the risk of lumbar spine injuries.

Hasson et al. (1980) measured the tolerance of 109 lumbar vertebrae including L1-L4 from 36 subjects with an average age of 58.5 years old (31 to 79 years) under axial compressive loads. It was observed that the overall tolerance of all vertebrae measured in the study was 2.63 ± 0.97 kN. More specifically, the tolerance of L1 to L4 were 3260 ± 211 kN, 3760 ± 280 kN, 4109 ± 347 kN, and 4807 ± 347 kN, respectively. It was

also reported that statistically there was no correlation between the vertebral level and the loading tolerance.

Myklebust et al. (1983) also tested the tolerance of lumbar vertebrae from subjects with an average age of 60 years (range of 34 to 78) by compressing individual vertebra. It was shown that the range of individual lumbar vertebra load tolerance ranged from 1957 to 7384 N, and the mean strength was 4972 N.

Yoganandan et al. (1988a) investigated the failure compressive load of spine vertebral bodies from T12 to L1. The mean failure force of individual vertebral bodies ranged from 2000kN to 5000kN. It was observed that there was no significant trend of failure force from T12 to L1; Yoganandan et al. (1988b) reported that the overall T12-L5 load tolerance under axial compression was 4.28 ± 0.34 kN.

Different from Hassonet al. (1980) and Yoganandan et al. (1988a), the tolerance of T10 to L5 measured in Brinckmann et al. (1989) showed a trend of decreasing from lower vertebrae to upper vertebrae. Moreover, the study found a correlation between areas of endplates and the failure load. It was observed that smaller areas of endplates were associated with less failure loads.

Stemper et al. (2018) utilized lumbar spine segments to quantify force tolerance of the lumbar spine. It was observed that the peak force of sub-failure and failure were from 2.6 to 7.9 kN and corresponding peak accelerations from 7 and 57g. The study also estimated the relationship between the load and the risk of injury of the lumbar spine.

3.3 Human Studies on the Effect of Musculature

Literature observed that occupants tend to brace before an upcoming impact (Hault-Dubrulle et al., 2009; Gao et al., 2015) and volunteers who tensed muscles had different kinematic responses from volunteers who kept relaxed during sled tests (Roberts and Carrol, 2003).

The smallest structural unit of muscle is the motor unit which contains a motor neuron and all muscle fibers controlled by this neuron. When stimulated, all fibers in this motor unit contract together (Lorenz et al., 2001). It was found that the muscle activation level varies under different loads. Nachemson et al. (1976) measured the pressures inside intervertebral discs and electromyography (EMG) of torso muscles when volunteers were stationary or performing lifts in different positions. It was observed that when the degree of backrest inclination increased (from 80 degrees to 130 degrees), the muscle signal at L3 decreased and so did the load on the intervertebral disc. This is because muscle contraction is not “all-or-none”. Although all fibers in each motor unit contract together, every motor unit is not active at the same time. The muscle activation level differs depending on the stimulation. The stronger the stimulation, the more motor units are activated leading to higher muscle contraction levels (Lorenz et al., 2001). This is important in understanding MVC studies because it was observed that occupants tended to brace to avoid upcoming impact during the MVC (Siegmund et al., 2014).

Hault-Dubrulle et al. (2010) investigated the responses of occupants from driving simulator tests mimicking an emergency situation of an abruptly appeared trunk in front of drivers' vehicle. When occupants realized the upcoming impact, they tend to brace and brake. As a consequence of bracing, occupants straightened arms and legs while

pushed trunk and pelvis back into seats. Therefore, forces on steering wheels and foot pedals increased.

Roberts and Carroll in 2003 measured EMG signal curves of main neck muscles in volunteer rear sled tests. It was observed that involuntary contraction of some muscles were potentially early enough to change the kinematic and kinetic responses of head and neck so that these early contractions might simulate or control whiplash injuries.

Tencer et al (2002) observed that although in low-speed frontal crashes the femur fracture was a major injury, external forces measured on the femur during reconstructed sled tests were below the fracture threshold. Adding estimated internal forces generated by lower extremities muscle contraction explained almost all femur fractures. Therefore, it indicated that lower extremities muscle contraction might increase the femur load and lead to fracture during low-speed frontal crash.

Eckner et al. in 2014 has already investigated the effect of activation timing on brain injuries. It was observed that anticipatory neck muscle contraction could reduce the risk of brain injuries during impacts.

Sharma et al. (2011) and Stilwell et al. (2016) reported real clinical cases that the seizure which induces uncontrollable muscle bracing of patients can lead to lumbar fracture. It suggested that during frontal crashes, lumbar muscles may also be able to generate enough force to break the lumbar spine.

All of the above has confirmed that muscle contraction can affect the risk of injuries. However, the effect of active muscle is not simulated when using cadavers as surrogates. Although the loads produced by neck muscles are represented by cables in

some ATDs (Martin et al., 2007), it could only partially account for an aware occupant. Therefore, another method has been gaining popularity and development: the finite element HBM.

3.4 Development of HBM

In engineering studies, many physical phenomena can be described by partial differential equations. It is almost unlikely to solve these equations by classical analytical methods. However, the finite element method (FEM) is a useful tool of a numerical approach to solve these equations approximately on the computer by simulations.

The basic theory of the FEM is to divide a body (object) into finite elements. The more elements, the more exact the solution is. But the computing time and cost increases as well. Therefore, it is optimal to build models with enough elements to produce approximate solutions, but not take too much computing time and cost (Fish and Belytschko, 2007).

The FEM is also widely used in automobile safety studies. As Osth mentioned in 2010, in order to understand the mechanism of crashes, it is common to reconstruct the crash partially or completely by the use of human surrogates, especially under injurious loading or vehicle crash speeds. Sometimes when a large number of tests are needed, numerical models are considered worthwhile because of the obvious financial benefits. The human body model (HBM) is one of the common types of FEM models used in vehicle crash research. The HBM is a numerical model that replicates human anatomical and physical properties and simulates the response of the whole human body. It can be the entire body model or a model of parts of the body. A good example of a segment

HBM is the lumbar spine model developed by Jaramillo et al. (2015). This lumbar spine model included L4, L5, sacrum, and intervertebral discs between each segment. It was validated and could be used to study the loading that occurs in MVC.

Yang et al. (2006) reviewed 50 years (up to 2006) of publications on HBMs published in the Stapp Car Crash Conference Proceedings and Journal. One of the early stages of the entire HBM using FEM was introduced by Huang et al. (1994). It developed a model of a 50th percentile male containing rib cage, shoulders and upper arms, pelvis and thighs, which were surrounded by muscles, ligaments and skin and had visceral content inside (**Figure 3-4-1 a**). It should be noted that since the goal of Huang et al.'s study was to develop a validated model emphasizing chest injuries, only the rib cage was refined. The vertebrae were only constructed by a few elements while the muscles were defined as a layer of membrane elements and the visceral content was defined as a viscous filling inside the trunk. The model was validated by sled tests and pendulum tests. It was shown that the model had a reasonable agreement with previous physical tests and could be used to predict chest injuries. Although as Huang et al. mentioned, this model needed to improve, but it did provide a good representation of human geometry.

Lizee et al. (1998) developed another HBM, also representing the 50th percentile of adult males. In this model, many body parts such as cervical, thoracic and lumbar spine were refined in detail but defined as rigid. The muscles in Lizee et al.'s model were defined as a layer of shell elements. Lizee et al. focused on the validation data found in the literature and validated the model by over 30 different published experimental studies such as isolated pelvis tests, thoracic belt compression tests, and neck tests. The

validation results showed the feasibility of the model to reproduce injury criteria and the physical quantities of human bodies such as forces. After this, more and more accurate models such as Ruan et al. (2005) and Kimpara et al. (2005) have been developed.

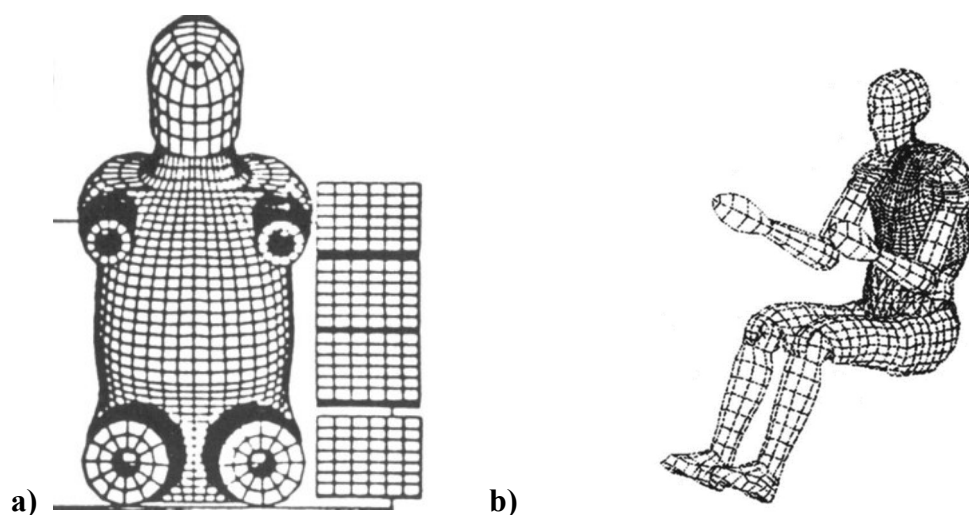


Figure 3-4-1: a) The model of Huang et al. (1994); b) The model of Lizee et al. (1998)

Researchers aim to not only develop passive HBMs, but also active HBMs which contain detailed active muscles in order to more accurately mimic human being's behavior with muscle contraction. Choi et al. (2005) developed an HBM with active muscles of upper and lower extremities and validated the model by volunteer sled tests. Eight volunteers of an average age of 24 were asked to brace their muscles in a sled test from the beginning of the descending until the sled stopped by barriers. EMGs of upper and lower extremities as well as loads on the foot pedal and the steering wheel were measured. The activation level of each muscle used in the HBM was the mean value of EMGs normalized by the maximum isometric voluntary contraction. The foot pedal and

steering wheel forces were also measured and compared to the volunteer test. The results showed that the model exhibited a good agreement with the experimental tests.

More recently, Gayzik et al. (2012) introduced a seated HBM produced by the GHBMC (**Figure 3-4-3**). The GHBMC was founded in 2006 and the Full Body Model (FBM) Centers of Expertise (COE) was officially founded in 2008 (Combest, 2018). It is an international consortium of automakers and suppliers working with research institutes and government agencies. The goal of the GHBMC is to develop and maintain high fidelity Finite Element human body models for automotive crash simulations to advance crash safety technology. The GHBMC HBM, as mentioned previously, is a series of HBMs used to predict behaviors of humans during blunt injuries such as vehicle crashes. The models were developed by an advanced general-purpose multi-physics simulation software package called the LS-DYNA® (LSTC, Livermore, CA). The GHBMC HBMs include simplified and detailed individual models and aged and obese model sets, as well as detailed pedestrians with various solvers (GHBMC) (Combest, 2016). **Figure 3-4-2** demonstrates the history of the development of the GHBMC HBMs until 2016:

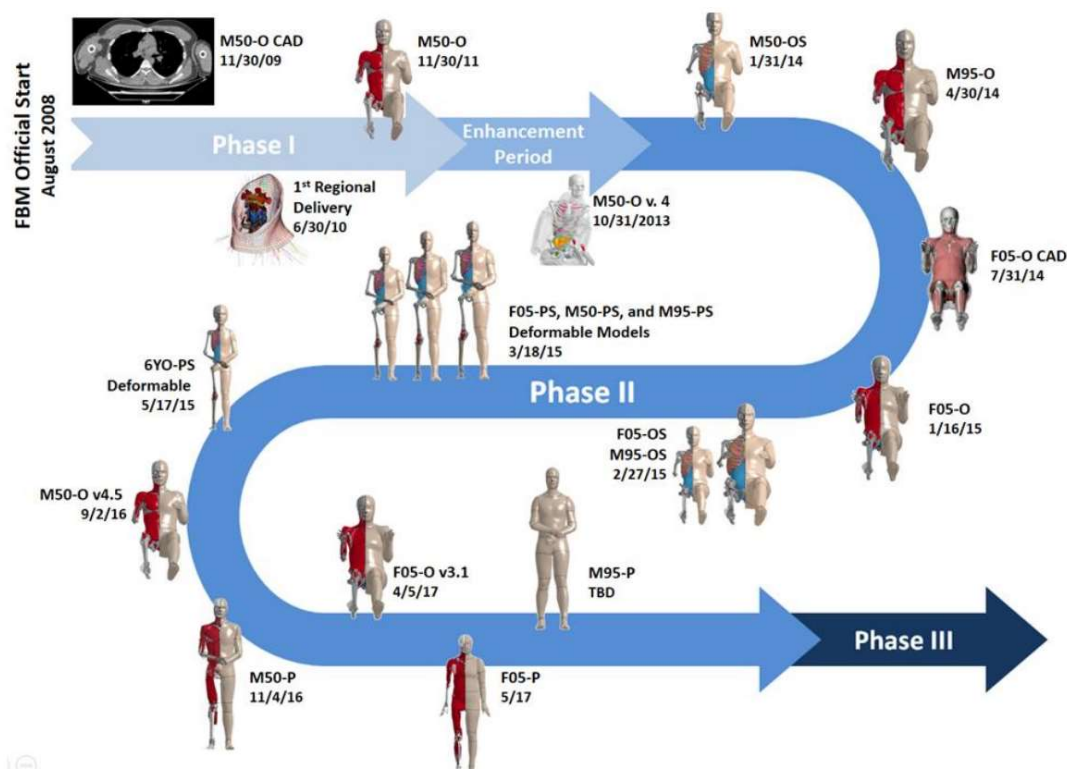


Figure 3-4-2: The history of the development of the GHBM HBM (Combest, 2016)

Among these models, the 50th percentile male (M50) detailed seating model, which will be used in the current study, was specifically described in Gayzik et al. (2012). The geometry of the M50 model was obtained from a 26-year-old healthy male volunteer with a height of 174.9 cm and weight of 78.6 kg. Clinical scanning methods including computer tomography (CT), magnetic resonance imaging (MRI), and upright MRI were utilized to collect the geometry of this volunteer, and Computer-Aided Design (CAD) was used to further develop anatomical details of the model (Gayzik et al., 2012).

The model was divided into parts and respectively developed by different Body Centers of Expertise (COE). Each part was then assembled to build the whole model. The requirements for types of elements varies depending on the material properties of human

body tissues. The muscles of the neck were modeled by three-dimensional hexahedral elements with one-dimensional elements within them. Abdominal muscles (rectus abdominis, obliques, erector spinae and quadratus Lumborum) and muscles of the pelvic region (psoas) were modeled by three-dimensional elements. It should be noticed that in the earlier version (V4.5), the lumbar spine was defined as a series of rigid body vertebrae and the intervertebral discs were modeled by 6-degree-of-freedom (DOF) beam elements. While in the newest version (V5.0), the lumbar spine is deformable and the intervertebral discs are modeled by layers: curve-defined anisotropic annulus, curve-defined fibrous and elastic fluid nucleus (Gayzik et al., 2012).

This M50 model was validated by several frontal and lateral impacts, two of which were a chest impact and an abdominal impact. As mentioned previously, it was reported that since the geometry of the model was obtained from a live volunteer and had been validated by over 20 impact tests, this GHBMC M50 has great potential to predict human response during vehicle impacts (Gayzik et al., 2012).



Figure 3-4-3: The Model of the GHBMC HBM detailed M50

3.5 HBM Studies on Effects of Muscle Contraction

The effect of musculature on kinematic and kinetic responses of human during an impact has been studied by many researchers.

Choi et al. (2005) investigated the effect of upper and lower extremities muscle contraction on the kinematic and kinetic responses of occupants utilizing the HBM. It was observed that bracing changed the response of occupants during an impact. The bracing driver tended to extend the elbows and knee joints, and therefore pushed the pelvis back into the seat.

Gao et al (2019) also found by utilizing the numerical HBM that in the model with active neck muscles, the head was stretched backward while no change was found

in the passive model. In addition, the head of the active model protracted to the end of the natural range earlier than the passive model.

Nie et al. (2018) investigated the influence of active lower extremities muscles on lower extremities injuries during knee airbag deployment. It was observed that the bracing occupants sustained high force on lower extremities when they impacted onto knee airbags. The bracing also induced high force between the foot and foot pedal. This is due to the increasing axial force on the femurs and tibias by the muscle of lower extremities during bracing.

Stemper et al. (2006) investigated the influence of early contracted neck muscles on neck whiplash injuries using a numerical head-neck model. It was reported that the early contraction highly restrained the motions of head and neck during an impact compared to relaxed model, and therefore potentially reduced the risk of neck whiplash injuries.

Jin et al (2017) investigated the effect of cervical musculature on head injury during an impact by using the GHBM HBM. The study constructed 4 simulations including: no activated; early activated; late activated; and stronger bracing. It was observed that active neck muscles could reduce the risk of brain injury. Moreover, the late activated simulation did not significantly reduce the risk of brain injury compared to the no activated simulation, whereas the early activated simulation did decrease the chance of brain injuries.

Although few studies focused on the effect of lumbar spine musculature on responses of occupants previously, all these HBM studies and human studies mentioned

in section 3.3 shows that the muscle factors such as activation level and timing of activation do play a role in the response of occupants, and lumbar musculature perhaps also affects the risk of lumbar spine injuries during the MVC.

3.6 Studies on the Effects of Crash Pulse

Epidemiological studies reviewed in the background chapter have already confirmed that the frontal central crash is a severe MVC as it induces a high risk of fatality and severe injuries.

Hong et al. (2008) investigated the relationship between the frontal crash types and the severity of crashes. The study constructed three numerical frontal crashes including a full-frontal crash; an offset frontal crash; and a frontal center pole crash to investigate the effect of different frontal crashes on the intrusion of occupant compartment and the deformation of a 2001 Ford Taurus. It was revealed that the frontal center pole crash had the highest intrusion of occupant compartment, especially the right toepan and the brake pedal. It was also observed that in the frontal center pole crash, the pole did not impact the frame rails, a construction at the front of vehicles to absorb energy during frontal crashes. Instead, the pole hit between frame rails into the front of the vehicle. The deformation was significantly more than the other two types of frontal crashes, which suggested a higher risk of injuries.

Kullgren et al. (2000) studied the relationship between crash pulse and neck injuries in frontal impact by investigating 187 occupants in frontal crashes. The study divided crash pulses into three phases: phase 1 of 0-33ms; phase 2 of 34-67ms; and phase 3 of 68-100ms. It was observed that a high mean acceleration in phase 2 and a low mean

acceleration in phase 3 might increase the risk of neck injuries. Although this trend may not be exactly the same as for lumbar spine injuries, it still demonstrated the influence of crash pulses on the human body injuries.

Tang et al. (2019) compared influences of different frontal crash pulse on the lumbar spine force by numerical method. The study utilized three frontal crash pulses with an initial speed of 35mph including: two pulses with an early sharp peak acceleration; a pulse with a late sharp peak acceleration; and a relative “soft” pulse. The results showed that the pulse with early peak acceleration induced the highest lumbar force, whereas the soft pulse gave the lumbar spine the lowest force.

Moreover, Hauschild et al. (2013) investigated the effect of full-frontal and frontal-pole crash deceleration pulse at the same initial speed on lumbar forces of dummies in frontal sled tests. It was observed that the deceleration pulse of frontal-pole crashes resulted in higher lumbar spine forces than the deceleration pulse of the full - frontal crash. In addition, by observing the deceleration pulses, it was observed that the frontal-pole crash pulses had higher and steeper peak deceleration.

Stigson et al. (2012) also observed that during frontal crashes, higher peak deceleration induced a higher risk of injuries of occupants, which in turn proved that the frontal pole impact could result in higher risk of injuries.

All these studies revealed that the frontal central crashes have steep crash pulses, and the steep crash pulse can induce a high risk of injuries. Therefore, in the current study, the deceleration pulse was selected for a frontal central crash.

In conclusion, HBM can investigate kinematic and kinetic responses of occupants in high-speed crashes without ethical concerns, and the GHBM HBM is one of those HBMs developed in recent years and has been used in many studies. Frontal central crashes are severe crashes whereby lumbar spine injuries are frequently observed, as mentioned in previous sections. Awareness of the upcoming impact and muscle contraction have been proven to affect the risk of injuries in other body regions, but the effect of lumbar musculature has barely been studied or reported in literature. Therefore, this study aimed to investigate the effect of lumbar musculature activation level and the timing of the activation in high-speed frontal central crash by using the GHBM

IV. FUNCTIONAL ANATOMY

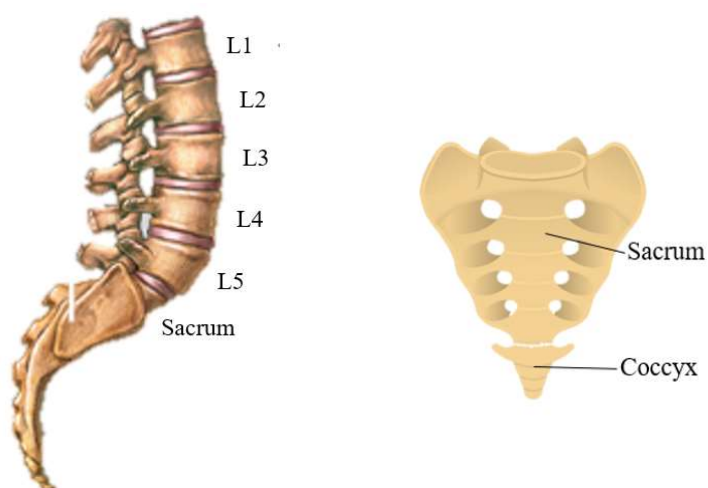
Five vertebrae (L1-L5) located vertically between the thoracic spine and the sacrum which are interconnected by soft tissues such as intervertebral discs, ligaments, and muscles, form the lumbar spine. The primary function of the lumbar spine is to support the weight of the head, neck, torso, and upper extremities thereby supporting physiological motions (Stemper et al., 2014). Below are major components of the lumbar spine:

4.1 Bony Vertebrae

Five lumbar vertebrae form a convex (or lordotic) curvature. A lumbar vertebra consists of an outer layer of dense and compact cortical bone, and an inner layer of porous cancellous bone. Posterior bony elements, including pedicles, transverse processes, articular processes, laminae, and spinous processes cooperating with the anterior vertebral body form a vertebral canal to protect the spinal cord and nerves. The flat, kidney-shaped vertebral bodies constitute the most massive portion of the lumbar spine and are larger in the lumbar region than in the cervical and thoracic regions (Stemper et al., 2014). Most of compressive forces in the longitudinal direction, sustained by the lumbar spine are resisted by the vertebral bodies and intervertebral disc, especially by the cancellous bone (Kurutz et al., 2012). Their larger size allows for higher loadings on vertebral bodies (Nordin et al., 2001).

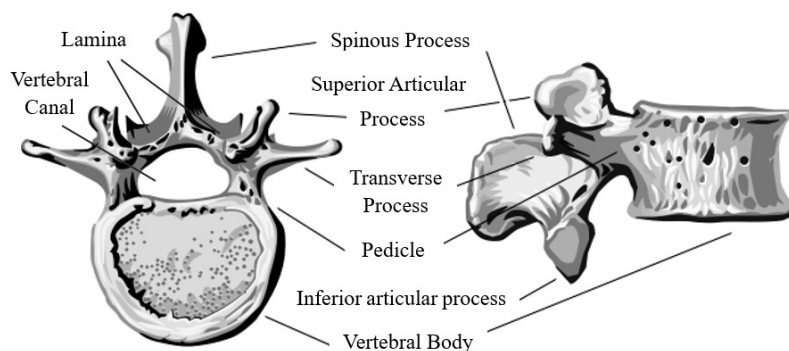
The sacrum, although not belonging to the lumbar region, is a common origin of trunk muscles, therefore it is also described here. For adults, the sacrum is a large,

triangular spinal bone fused from five infantile segments. It connects the inferior surface of L5 and the top of the coccyx and is central curved to form the upper and back portion of the pelvic cavity. Beside the origins and insertions of some trunk muscles, the sacrum also functions to maintain hip stability (Gray, 1918).



(Adapted from the U.S. National Library of Medicine and getbodysmart. com)

Figure 4-1-1: Lumbar spine and sacrum



(Adapted from Gray, 1918)

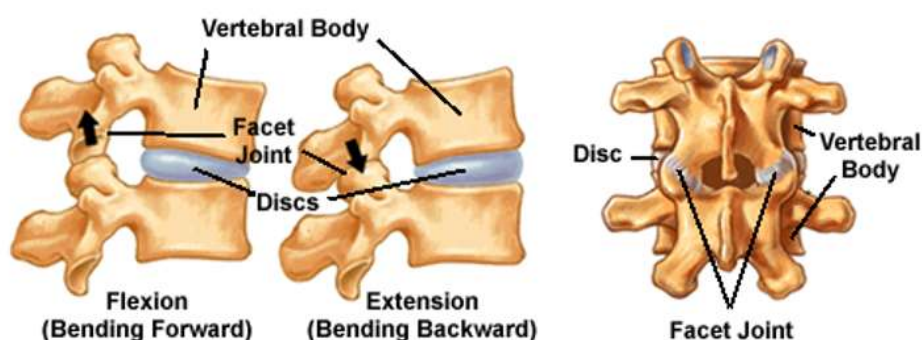
Figure 4-1-2: Lumbar vertebra

4.2 Endplates

Endplates are bony segments fused to inferior and superior of vertebral bodies and connecting to the intervertebral discs, which is introduced in the next section. Small pores in the endplates allow nutrition to be transported into the intervertebral discs (Nordin et al., 2001; Stemper et al., 2014).

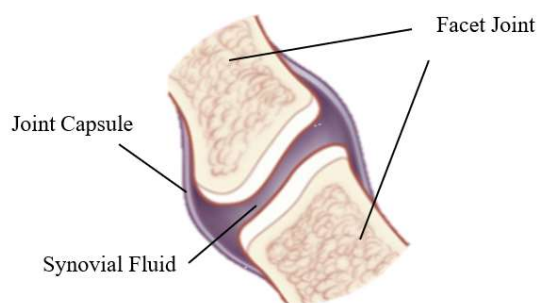
4.3 Facet Joints

The facet joint is formed between two adjacent vertebrae (T12/L1 to L5/Sacrum). It is formed by the inferior articular process of the upper vertebra and the superior articular process of the lower vertebra as in **Figure 4-3-1**. The facet joint is surrounded by a joint capsule and capsule ligaments. The synovial fluid inside the joint capsule allows opposing articular processes of facet joint to slide with each other during motions such as flexion and extension, lateral bending, and axial rotation (Stemper et al., 2014).



(Adapted from the Colorado Comprehensive Spine Institute)

Figure 4-3-1: Facet joints

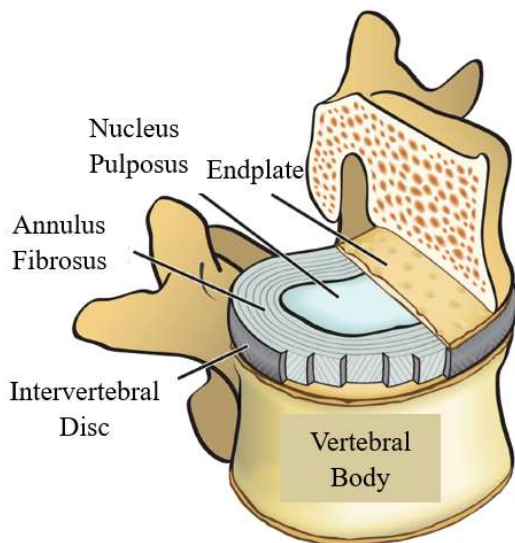


(Adapted from the Weill Cornell Brain and Spine Center)

Figure 4-3-2: Components of the facet joint

4.4 Intervertebral Discs

Intervertebral discs, the discs of soft tissue connecting adjacent vertebrae by endplates, consist of three layers: outer layers - annulus fibrosus formed by collagen fibrous rims and fibrocartilage inside; center-nucleus fibrosis made of collagen matrix and water; the transitional region between the annulus and nucleus fibrosis (Stemper et al., 2014). The functions of intervertebral discs are to bear and distribute loads, and to prevent extreme motions. In daily activities, the intervertebral discs are commonly subjected to a combination of the compression, bending, and torsion. Spinal flexion, compression, and lateral flexion usually produce tensile and compressive loads on the intervertebral discs, while rotation commonly generates shear forces (Nordin et al., 2001).



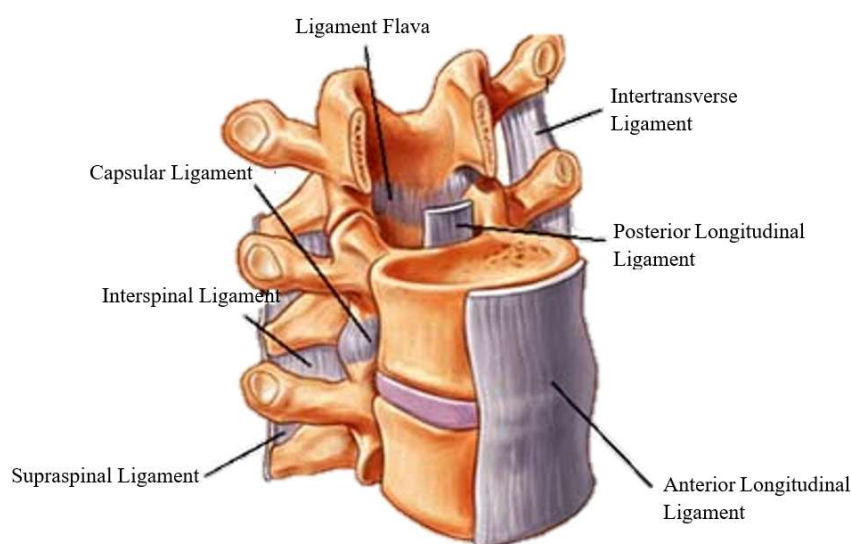
(Adapted from the Neupsy Key)

Figure 4-4-1: Intervertebral discs and endplates

4.5 Ligaments

The ligaments consist of collagen fibers that add strength and elastin fibers that add elasticity to the ligaments. There are generally 7 types of spinal ligaments in the lumbar region: anterior longitudinal ligaments (ALL), posterior longitudinal ligaments (PLL), ligamentum flavum (yellow ligaments), capsular ligaments, intertransverse ligaments, supraspinous ligaments, and interspinous ligaments (Gray, 1918; Stemper et al., 2014). All these ligaments except the ligament flava contain a high portion of collagen, which limits their ability of elongation during spine motions. The ALL is a broad ligament extending along the anterior vertebral bodies from the axis to the sacrum. The ALL is active during spinal extension and rotation. It also prevents hyperextension and excessive distraction. The PLL within the vertebral canal extends along the posterior vertebral bodies from the axis to the sacrum. The function of the PLL is to stabilize the

spine during flexion. The ligament flava, a series of ligaments from C2/C3 to the sacrum to connect the laminae to adjacent vertebrae, have a high elastin content. This high elasticity allows the ligament flava to assist laminae in returning to their rest position after flexion. The capsular ligaments connect opposing articular processes within facet joints. Their functions are to limit distraction and excessive sliding between two articular processes of a facet joint. The intertransverse ligaments are discontinuous and connect transverse processes of adjacent vertebrae. During the lateral flexion, the intertransverse ligaments sustain the highest strain. Finally, the supraspinous ligaments connect apices of the spinous processes from the C7 to the sacrum, whereas the interspinous ligaments located anterior to supraspinous ligaments connect the spinous processes and extend from the root to the apex of each spinous process. These ligaments stabilize the spine during lateral flexion (Gray, 1918; Nordin et al., 2001; Stemper et al., 2014).



(Adapted from www.spineuniverse.com)

Figure 4-5-1: Spinal ligaments

4.6 Muscles

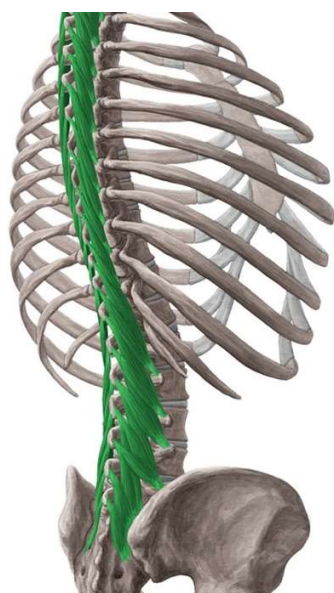
Skeletal muscles are the most abundant tissue in the human body (Stemper et al., 2014). The muscle fiber is another term for the muscle cell because of its spindle shape. A single skeletal muscle consists of a bundle of muscle fibers. The skeletal muscle is wrapped and divided into muscle compartments by a layer of connective tissue called the deep fascia. Immediately underneath this layer is a layer of collagen tissue named the epimysium. The muscle is further divided by the perimysium. Each muscle fiber is covered by the endomysium. A cylindrical or sheet-like tendon attaches the muscle to the bone. All these connective tissues are called the series of elastic elements (Saladin et al., 2018).

Anatomically, the muscle functional unit is the sarcomere. Each sarcomere has two types of filaments: the thick filaments which contain proteins called myosin, and the thin filaments containing numbers of proteins called actin and smaller amounts of troponin and tropomyosin. The muscle contracts by shortening the sarcomere. When the muscle is stimulated, the myosin head attaches to the actin filament and moves the actin filament forward. This motion shortens the sarcomere and further shortens the muscle (Saladin et al., 2018).

Muscles in the lumbar regions can contract to stabilize the lumbar spine (Stemper et al., 2014fish). The muscles involving lumbar spine motions can be divided into either erectors such as multifidus and erector spinae, or flexors such as quadratus lumborum, rectus abdominis, external abdominal oblique, internal abdominal oblique and psoas major (Gray, 1918; Nordin et al., 2001).

4.6.1 Multifidus

The multifidus is a group of deep back muscle attaching to the spinous processes and arising from the sacrum and iliac to the axis. In the lumbar region the multifidus origins from all mammillary processes, whereas in the thoracic region the multifidus origins from all transverse processes. When bilaterally contracting, the multifidus extends the spine; and when unilaterally contracting, the multifidus ipsilaterally flexes and contralaterally rotates the spine (Gray, 1918; Kenhub, n.d.).



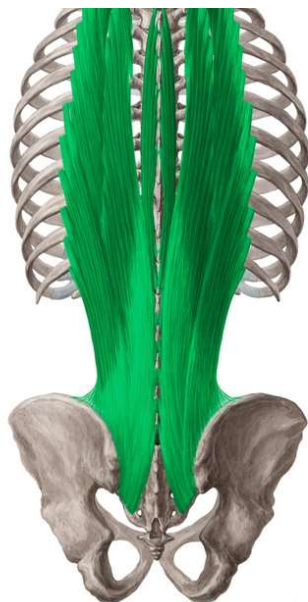
(Adapted from www.kenhub.com)

Figure 4-6-1-1: Multifidus

4.6.2 Erector Spinae

The erector spinae is a large back muscle which arises from the sacrum and is divided into subgroups as it travels upward through the whole spine. The function of this

muscle is to extend the spine by contracting bilaterally and to laterally bend the spine by contracting unilaterally (Gray, 1918; Kenhub, n.d.).

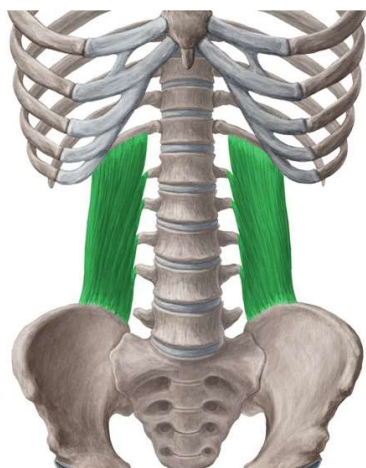


(Adapted from www.kenhub.com)

Figure 4-6-2-1: Erector spinae

4.6.3 Quadratus Lumborum

The quadratus lumborum, an irregular-shaped flexor muscle, originates from the iliac crest and inserts into the 12th rib and transverse processes of L1 to L4. This muscle acts to pull down the 12th rib. When the thorax and the vertebral column are fixed, the quadratus lumborum may raise pelvis to one side by contracting unilaterally, and flex trunk by contracting bilaterally (Gray, 1918).

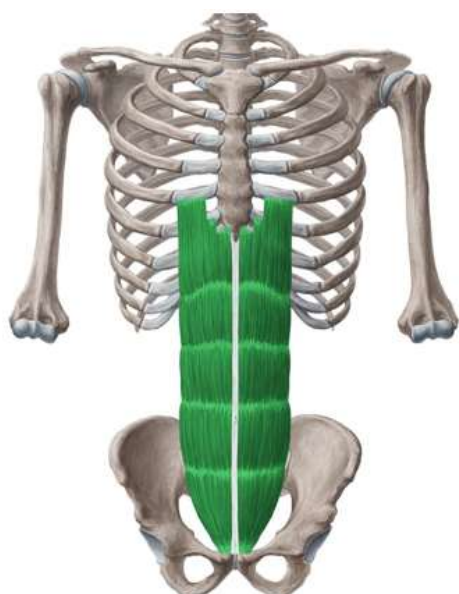


(Adapted from www.kenhub.com)

Figure 4-6-3-1: Quadratus lumborum

4.6.4 Rectus Abdominis

The rectus abdominis is a large flat abdominal muscle arises from the pubic crest and inserts to the cartilages of 5th, 6th and 7th ribs. The rectus abdominis acts as a flexor of the trunk.

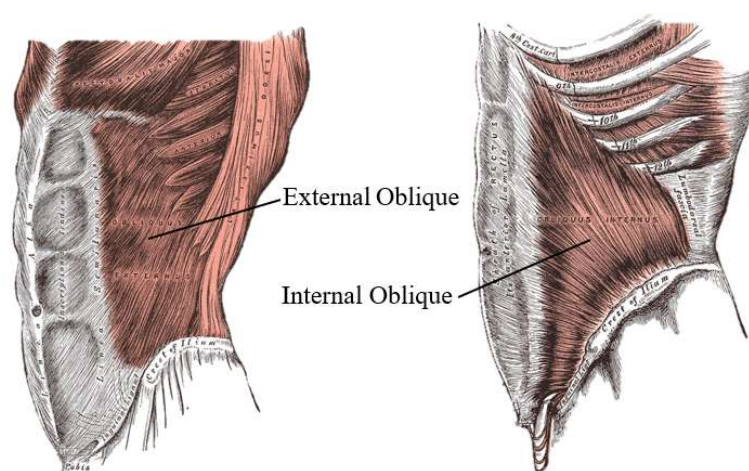


(Adapted from www.kenhub.com)

Figure 4-6-4-1: Rectus abdominis

4.6.5 External and Internal Oblique Muscles

The external oblique muscle is the most superficial abdominal flexor. This flat, broad muscle originates from the iliac to the costal cartilage. The internal oblique muscle, which lies beneath the external oblique muscle, also originates from the iliac and inserts into the costal cartilage. These two muscles flex the trunk when contract (Gray, 1918).

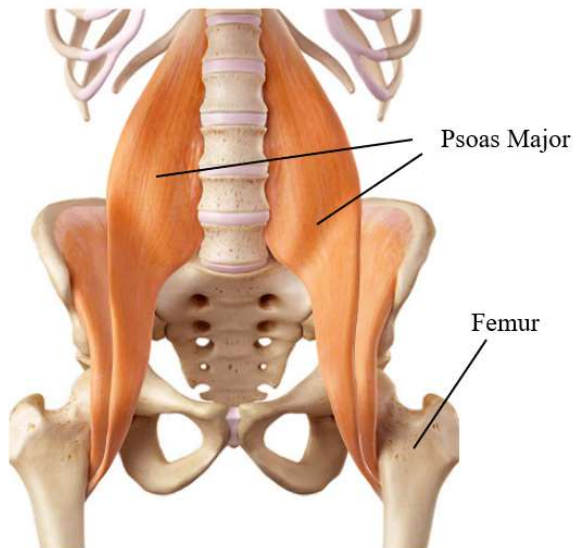


(Adapted from Gray (1918))

Figure 4-6-5-1: External and internal oblique muscles

4.6.6 Psoas Major

The psoas major is a significant deep muscle. It arises from the T12 and lumbar spine, travels downward crossing the pelvis, then proceeds in front of the hip joint, and finally inserts into femurs. Although the psoas major is usually considered a lower extremities muscle, as it originates from the spine and acts to flex the trunk, it is also recognized as a trunk flexor (Gray, 1918).



(Adapted from www.quizlet.com)

Figure 4-6-6-1: Psoas major

V. METHODS

5.1 Hill-type Muscle Model

The active trunk muscles in this study were constructed by 1D beam elements. The theoretical model representing how a beam elements mimics active muscle functions in alive human beings is the Hill-type muscle model. **Figure 5-1-1** below is a classic Hill-type muscle model.

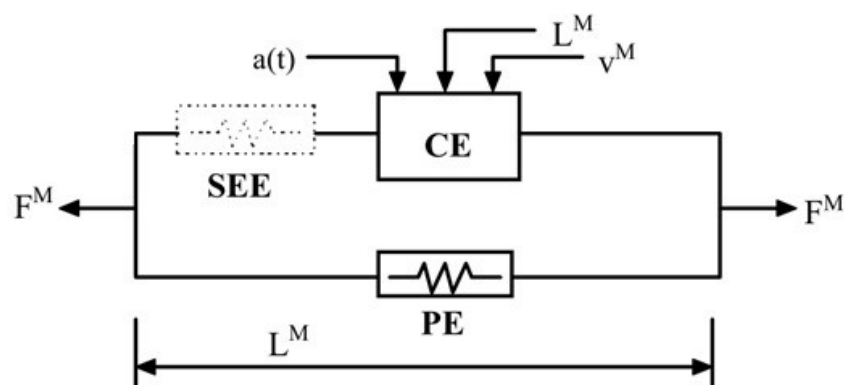


Figure 5-1-1: A classic Hill-type muscle model (Adopted from LS-DYNA Manual Volume 2)

A Hill-type muscle model consists of three parts: a contractile part (CE) which represents active properties of a muscle; a parallel part (PE) which stands for passive soft tissue properties; and a series part (SE) which represents tendons properties and is usually neglected. The total force generate by an active muscle, as shown in the figure, mainly depends on parameters: $a(t)$ from 0 to 1 to represent muscle activation level from

no activation at all to fully activated; L^M to represent the current length of an active muscle; and V^M to represent the current shortening velocity of the active muscle.

Since the GHBMC HBM used in this study already had 3D passive trunk muscles with tendons included and this study mainly aimed to understand the effect of active muscles on lumbar spine injuries, this study only considered the contractile part in active muscles.

The force generated by an active muscle as per the Hill Type material formulation can be expressed as:

$$F=F^{CE}=a(t) \times F_{\max} \times f_{TL}(L) \times f_{TV}(V)$$

$$L=L^M/L_0$$

$$V=V^M/(V_{\max} \times S_v[a(t)])$$

where $a(t)$, as mentioned previously, represents muscle activation. In this study, $a(t)$ is a curve wherein activation level varies with time; F_{\max} is the maximum force an active muscle can generate and is equal to the product of the maximum isometric stress (σ_{\max}) and the physiological cross-sectional area (PCSA) of a muscle; L , the normalized length which is automatically calculated by the LS-DYNA, is the ratio of the current length (L^M) of an active muscle and the initial length (L_0) of that muscle. In this study, σ_{\max} was 0.5MPa as consistent to Osth (2010) and within the range recommended by Winters (1995). f_{TL} is determined by a normalized tension (f_{TL}/F_{\max})-normalized length curve which was recommended by Winters (1995) as shown in **Figure 5-1-2**; V , the normalized shortening/lengthening velocity which is also automatically calculated by the LS-DYNA, is represented by the maximum velocity (V_{\max}), the current muscle velocity

(V^M) and a parameter S_v which either varies with the $a(t)$ or is defaulted to 1 as in this study. Winters (1990) recommended the range of velocity from $2 l_{orig}/s$ to $8 l_{orig}/s$ for muscle fibers from slow fibers to fast fibers. Since the ratio of fast to slow fibers in trunk muscles are unknown, the V_{max} was selected as $5 l_{orig}/s$ in this study. f_{TV} is determined by the curve of normalized tension (f_{TV}/F_{max})- normalized velocity which was recommended by Winters (1995) as **Figure 5-1-2**.

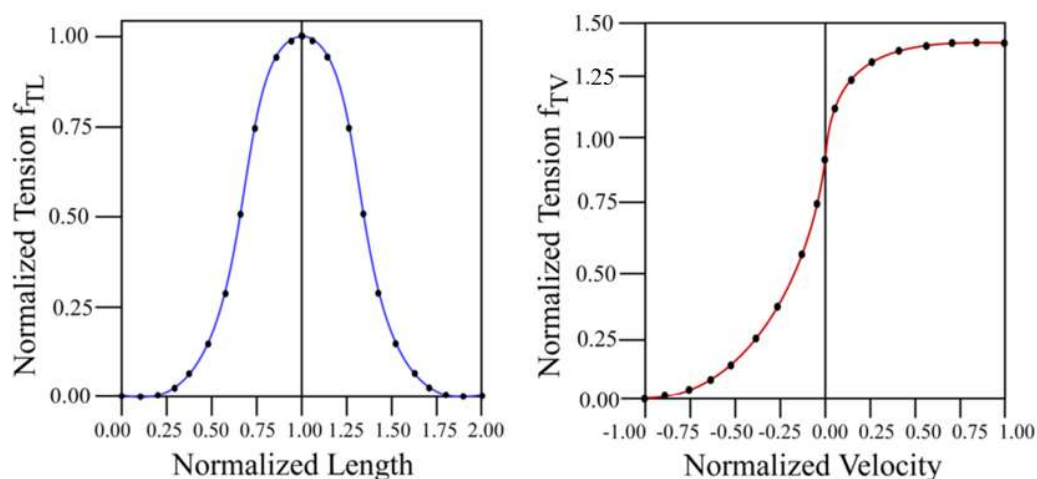


Figure 5-1-2: Force-length and force-velocity curves (adopted from LS-DYNA Manual Volume 2)

5.2 Implementation of the Musculature

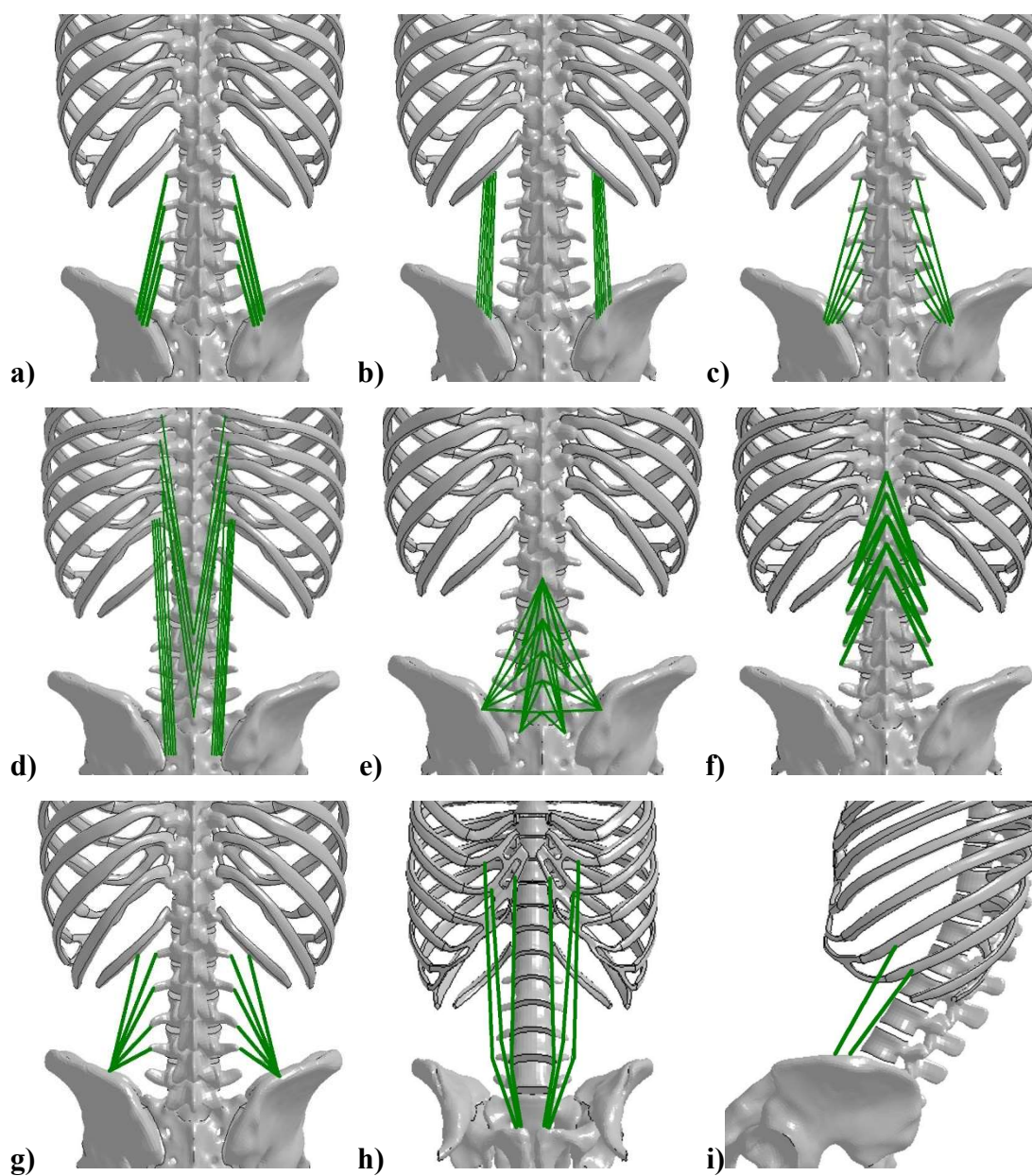
This study aimed to investigate the effect of muscle activation level and the timing of muscle activation on the kinematic and kinetic responses of occupants during a high-speed frontal crash. The simulations were run using LS-DYNA (LSTC, Livermore, CA). Since the newer version (V5.0) of the GHBMC HBM M50 was released in 2019, both the V4.5 and V5.0 were used in this study. The GHBMC HBM used in this study

had active and passive neck muscles, and passive trunk (thoracolumbar and abdominal) muscles such as psoas major, erector spinae, quadratus lumborum, and external oblique. The GHBM HBM itself did not include active trunk musculature. Therefore, the first step was to implement active muscles into the human body model. In order to closely mimic real human body behavior, the lumbar spine muscles, the thoracic muscles, abdominal muscles, and muscles of the pelvis region were implemented. Every muscle was broken into muscle elements and the origins and insertions of most muscle elements were obtained from Osth (2010), (**Table 1** in Appendix). The psoas major is normally considered as a lower extremities or hip-region muscle, and the active psoas major was not implemented on the model in Osth (2010). However, as the origins of the psoas major are mainly on the lumbar spine, and a part of its function is to flex the trunk, this active muscle was implemented in this study (Bogduk et al., 1992; Siccardi et al., 2020).

Eleven muscles, including 136 muscle elements were implemented on the GHBM HBM M50. These groups of muscles were erector spinae iliocostalis lumborum pars thoracis; erector spinae iliocostalis lumborum pars lumborum; erector spinae-longissimus thoracis pars lumborum; erector spinae-longissimus thoracis pars thoracis; multifidus lumborum; multifidus thoracis, quadratus lumborum muscles; rectus abdominus; external oblique muscles, internal oblique muscles, and psoas major. Each muscle was constructed by 1D beam elements. The muscle mass density was 1.06 g/cm^3 (Ward and Lieber, 2005). The material property was defined using the Hill-type muscle (material property of MAT_MUSCLE in the LS-DYNA) as described above. Input parameters are shown in **Table 5-2-1**.

Table 5-2-1: Parameters of the Hill-type muscle model in this study

Parameter	Value	Reference
Mass density	1.06 g/cm ³	Ward and Lieber, 2005
σ_{\max}	0.5MPa	Winters, 1995; Osth, 2010
V_{\max}	5 l_{orig}/s	Winters, 1990



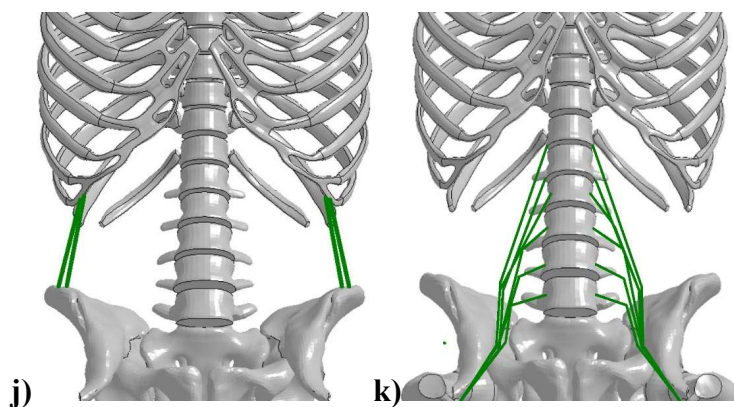


Figure 5-2-1: Trunk extensors: **a)** Erector spinae iliocostalis lumborum pars thoracis; **b)** Erector spinae iliocostalis lumborum-pars lumborum; **c)** Erector spinae longissimus thoracis pars lumborum; **d)** Erector spinae longissimus thoracis pars thoracis; **e)** Multifidus lumborum; **f)** Multifidus thoracis; Trunk flexors: **g)** Quadratus lumborum muscles; **h)** rectus abdominus; **i)** External oblique muscles; **j)** Internal oblique muscles; Lower extremities muscle: **k)** Psoas major

5.3 Validation

Ejima et al. (2007) investigated kinematic responses and muscle activations of occupants during a simulated frontal crash by utilizing low-speed frontal sled tests with human volunteers. The sled setup consisted of a rigid seat, mounted on a 10-degree ramp. The sled was accelerated by gravity and hit a damper at the end of the rail around 200ms to simulate passengers applying emergency brakes. Three healthy male volunteers (23 years old) were selected for the experiment. The volunteers were restrained by a non-pretensioned lap belt and leg belt. The volunteers were instrumented with markers on the top of the head, the head center of gravity (head CG), T1, T12, pelvis (marked on the iliac crest), etc. Cameras were set up to capture motions of those markers. Volunteers were asked to keep a relaxed posture during the test. The excursions of head top, head CG, T1 and T10 relative to the pelvis were extracted by processing the volunteer motions from video images.

The EMG signals of the major muscles, such as sternocleidomastoid, paravertebral muscle (neck), erector spinae, rectus abdominis, and obliquus externus abdominis muscles, were measured and then normalized by the maximum EMG value of the same muscle which was measured by asking the volunteer to brace the whole body. Thus, values for the normalized EMG signal curves between 0 to 1 were reported in the study.

To validate the GHBM HBM implemented with muscles of the current study, the HBM implemented with new muscles was applied in the similar sled test as in Ejima et al. (2007). The simulation environment consisting of a rigid seat with seat pan and backrest, and a footrest was developed. The GHBM HBM was positioned on the seat and restrained by a lap belt. The lower extremities of the HBM were tied with a leg belt similar to what was done with the volunteers. Contacts between the HBM and the environment were defined. The deceleration pulse of around 1g shown below from Ejima et al. (2007) was applied to the seat as the boundary condition.

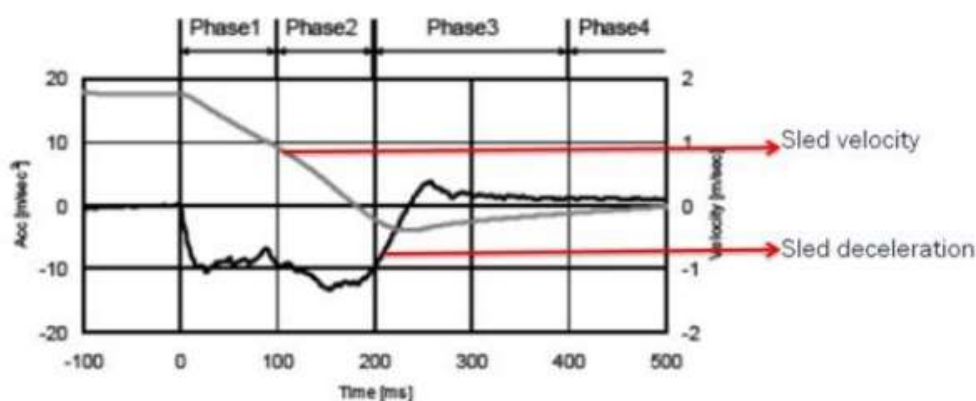


Figure 5-3-1: Deceleration pulse (Ejima et al., 2007)

Five cases in total were simulated using the GHBM V4.5 and V5.0 HBM each. Active neck muscles which have already been developed in the GHBM HBM previously were also simulated in the same way as trunk muscle in the validation except for the case without active muscles, which will be described in detail in the next paragraphs. Therefore, the “active muscles” mentioned in all contents below were not only restricted to new active muscles implemented by this study, but also active neck muscles already developed in the GHBM HBM.

The first two cases simulated as baselines were 1) case 1: HBM implemented with active muscles but no activation was simulated (passive response); 2) case 2: HBM without any active muscles at all. As only the CE was considered in this study, the excursions of these two cases should be similar. These two cases were simulated to confirm this theory as well.

The remaining three validation cases were based on the EMG signal data reported by Ejima et al. (2007). The EMG signal curves of sternocleidomastoid; paravertebral muscle; erector spinae; rectus abdominis; and obliquus externus abdominis muscles were measured in the experiment. In case 3 every muscle which was measured in the experiment used the activation level curve of the same muscle from the experiment. Since only a few superficial muscles were measured by the experiment, other superficial and all deep muscles in HBM used the same EMG signal curves of muscles that were close to the measured muscles. For example, in the cervical region, neck flexor anterior scalenes used the same curve of sternocleidomastoid; the trunk flexor internal oblique used the same curve as the external oblique.

After observing the results of case 3, it was shown that the body segment excursions of the GHBMC HBM did not have a good agreement with the results of the experiment (will be discussed in the results and discussions); and as no deep muscle was measured in Ejima's study, deep muscle activations in case 3 were only estimated. Therefore, to try to speculate activations level of deep muscles that were not measured in the experiment but were involved in this study, case 4 and case 5 were developed to adjust activations of deep muscles not measured in the experiments.

Case 4 was adjusted based on Astfalck et al. (2010). No other study was found to report the EMGs of thoracolumbar muscle activations during volunteer sled test of frontal impact as Ejima's, therefore in order to adjust muscle activations in case 4, a study measuring trunk muscle activation of volunteers during a relaxed sitting position, which was similar to Ejima's volunteer position, i.e. a relaxed sitting position, before hitting the damper, was considered. Astfalck et al (2010) measured muscle activations of volunteers during the regular relaxed sitting position, including multifidus (superficial multifidus), thoracic erector spinae, internal oblique (transverse fibers), and external oblique (Astfalck et al., 2010). It should be noted that the multifidus and internal oblique muscles were deep muscles, but Astfalck's study measured these two muscles by the method mentioned in Dankaerts et al. (2006). The surface electrodes of internal oblique were placed at "*1 cm medial to the anterior superior iliac spine (ASIS) and beneath a line joining both ASISs*"; the surface electrodes of multifidus were placed at "*L5 and aligned parallel to the line between the posterior superior iliac spine (PSIS) and the I1-I2 interspinous space*" (Dankaerts et al., 2006). The EMG signal curve of each muscle of

every volunteer was normalized by using the existing standard of submaximal voluntary isometric contraction (sub-MVIC). Then for each muscle, the means of data from all volunteers' normalized EMG signal curves during a relaxed sitting position was calculated and reported as the mean muscle activation of each muscle during a relaxed sitting position. In the current study, by comparing these mean muscle activations during a relaxed sitting position from Astfalck et al. (2010), it was found out that the mean muscle activation of the multifidus (deep trunk extensor) was around 50% as the thoracic erector spinae (superficial trunk extensor); the mean muscle activation of the internal oblique (deep trunk flexor) was around 150% as the external oblique (superficial trunk flexor). Therefore, in case 4 for all active muscles, muscle activations of deep extensors were reduced to 50% as it was in case 3; muscle activations of deep flexors were scaled to 150% as it was in case 3. The superficial muscles were kept the same as in case 3. Then the simulation of case 4 was run to see if results were improved. This will be discussed in the results and discussions.

Besides case 4, another thought to adjust deep muscle activations was applied in case 5 at the same time. As only superficial muscles were measured in Ejima's study, case 5 simulated only superficial muscles as well. Deep muscles were not removed but set as no activation. The simulation of case 5 was also executed to observe if any improvement in the body segment excursions resulted. This will also be mentioned in the results and discussions.

The EMG signal curves were first digitized as forms by the Origin (OriginLab Corporation, Northampton, Massachusetts, USA) and then used as an input to activate

the muscles. **Table 1** in the appendix shows origins, insertions, functions, muscle layer classifications, PCSAs, lengths, and activation level curves of muscles trunk muscles implemented in this study.

The simulations were analyzed for head top, head CG, T1, and T10 excursions relative to the pelvis and were compared with experimental responses.

To make it simple, case 1 to 5 will also be called as: “no activation at all”; “without muscle”; “relaxed original”; “relaxed adjust”; and “relaxed superficial only” in the results and discussion when talking about the validation.

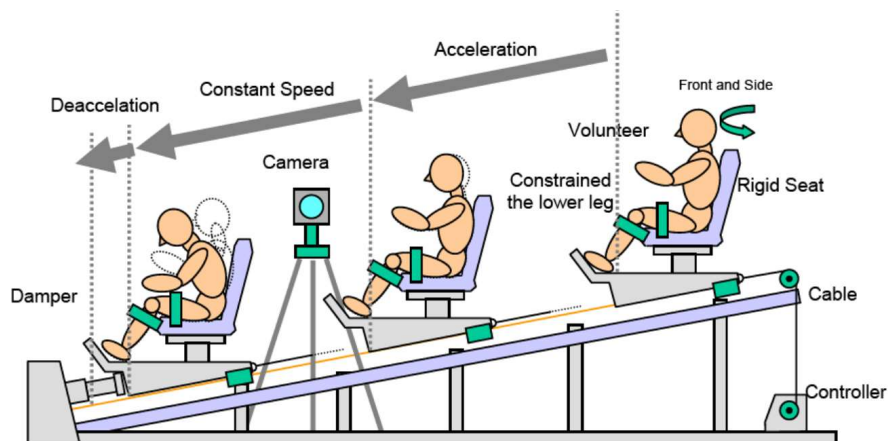


Figure 5-3-2: Sled test from Ejima et al. (2007)

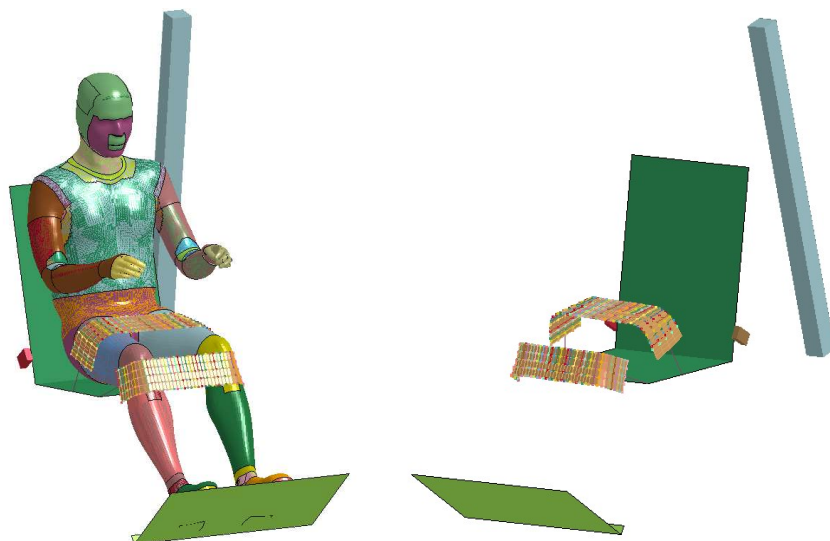


Figure 5-3-3: Setup of the validation

5.4 Investigation of the Effect of the Musculature in the High-speed Frontal Crash

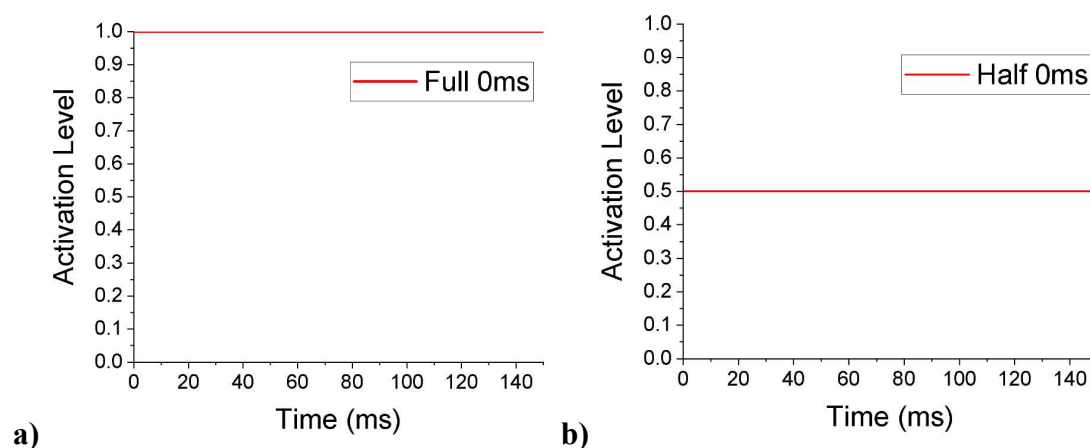
After the validation, the HBM was simulated in a high-speed frontal crash environment to understand the effect of bracing (muscle activation) and awareness (timing of the muscle activation) on lumbar spine forces. The simulation setup was extracted from a vehicle model (Toyota Yaris (2010)). The environment consisted of the vehicle seat with a deformable seat pan, backrest, B-pillar, the footrest, steering wheel and column, steering wheel airbag and deformable knee bolster. The HBM was restrained in the seat using a 3-point seatbelt. The 3-point seatbelt was attached to the B-pillar by an anchor. The part of the seatbelt contacting with the HBM was built by shell elements while the remaining parts were constructed by 1D belt elements. The retractor and the pretensioner were included in the model as well. The seat, B-pillar, and footrest were constrained to minimize relative motion between the structures. The timing of steering wheel airbag deployment was set at 20ms as it usually takes 15-40ms for an airbag to deploy after sensing an impact, and the deployment cannot be too early or too late to protect occupants (Phen et al., 1998). Hands positions of the GHBMC HBM were modified to mimic a posture of holding the wheel.

Sixteen cases in total were set up for the two HBM versions (V4.5 or V5.0) by varying the muscle activation level and the timing. The test matrix are shown in **Table 5-4-1**. All active neck muscles and active muscles developed in this study were used except for the simulations without muscles. The muscle activation was varied as fully activated, half activated, and not-activated. As no muscle activations during the high-speed frontal crash were reported, this study assumed that the muscle activation

increased from 0 at 0ms and reached the peak activation at a specific time point, then kept constant until the end of the simulation. The muscle peak activation level of each group was 1, 0.5, and 0, respectively as shown in **Figure 5-4-1**. The fully activated simulations represented occupants bracing their muscles strongly and the no activated group simulated occupants in a thoroughly relaxed stage, while the half-activated simulations represented the occupants activating their muscles incompletely. There was also a simulation without muscle as a baseline to investigate if the musculature did play a role in the frontal crash. The timing of activation was varied as 0ms (occupant realized the impact early), 40ms (occupant realized the impact late), and 80ms (unaware occupant). Below is a matrix of these 16 simulations, and muscle activation curves are shown in **Figure 5-4-1**:

Table 5-4-1: Test matrix

GHBMC HBM V4.5/V5.0			
Muscle activation level	Timing of the peak activation		
1 (fully activated)	0ms	40ms	80ms
0.5 (half activated)	0ms	40ms	80ms
Active muscles with 0 activation (no activation)			
without active muscles (without muscles)			



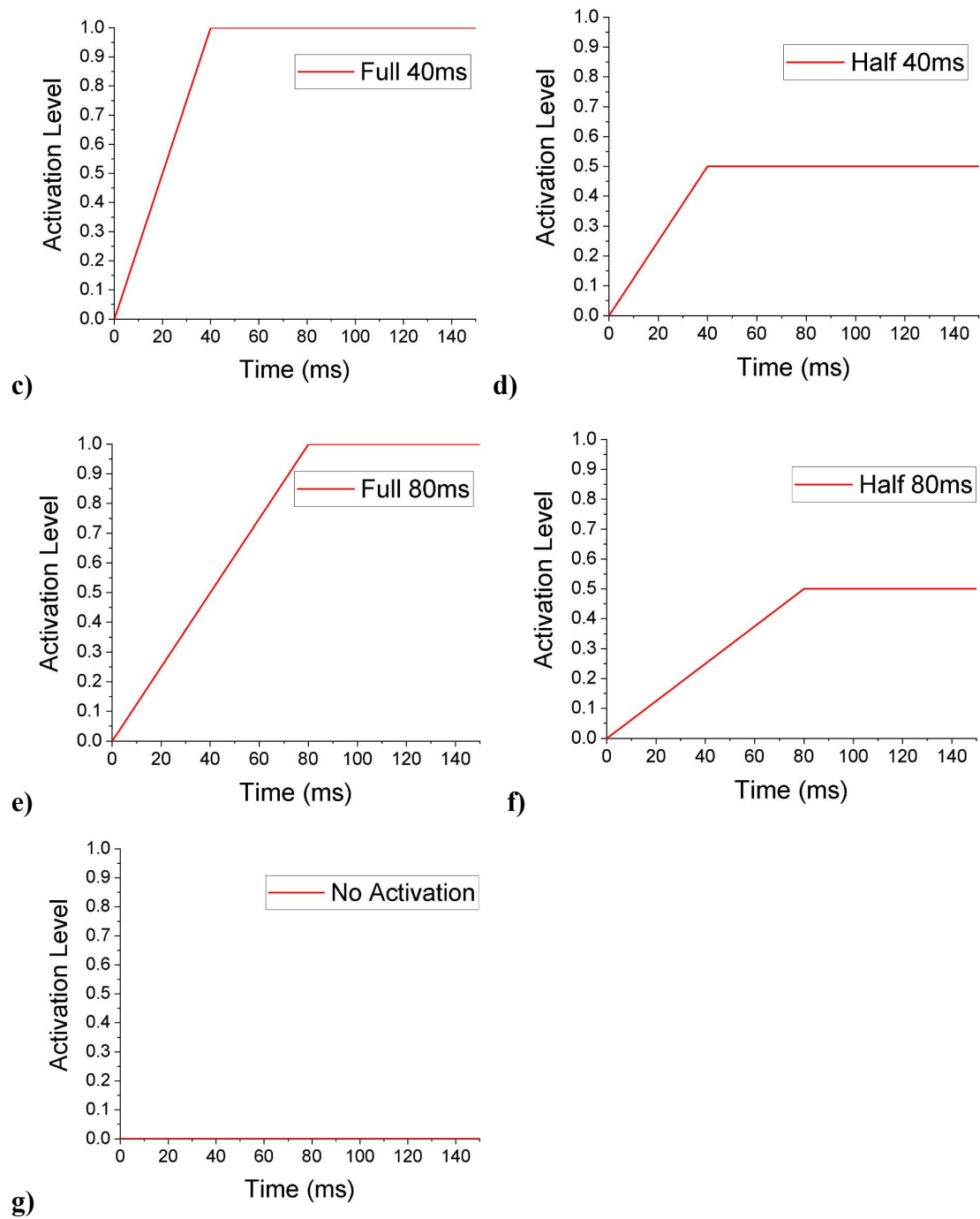


Figure 5-4-1: Activation level curves used in high-speed frontal crash simulations: **a)** Fully activated at 0ms; **b)** Half activated at 0ms; **c)** Fully activated at 40ms; **d)** Half activated at 40ms; **e)** Fully activated at 80ms; **f)** Half activated at 80ms; **g)** No activation

In conclusion, both V4.5 and V5.0 had 8 simulations, including fully activated at 0ms, 40ms, 80ms; and half activated at 0ms, 40ms, and 80ms. The deceleration pulse

was obtained from a real crash documented in the NHTSA (Toyota yaris, 2010) and was applied to the rigid structure of the vehicle. The initial speed was 56km/h as 73% of frontal crashes had an initial speed under 56km/h (Pintar et al., 2012), and each simulation was executed for 150ms. The compressive force (force in z-direction) curves loading on L1, L3, and L5 were measured from each simulation and the peak compressive force was compared to represent the effect of bracing during a frontal crash.

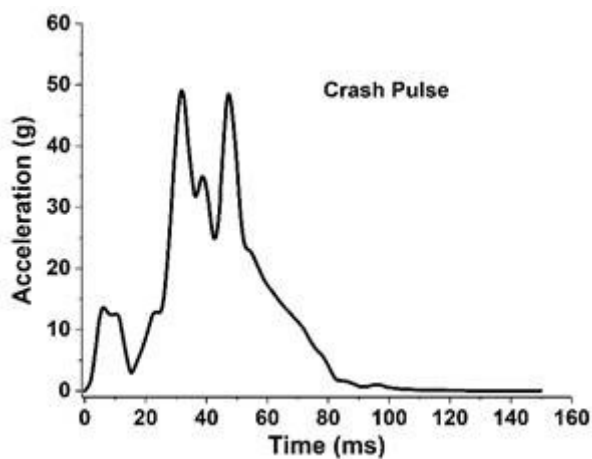


Figure 5-4-2: Acceleration pulse (Marzougui et al., 2013)



Figure 5-4-3: Outlook of the seated GHBMC HBM M50 in the vehicle

VI. RESULTS

6.1 Validation

This section presents results of validation by comparing excursions of volunteers in sled tests from the literature to the GHBMC HBM in the similar scenario. 5 cases for each version including: case 1: GHBMC HBM implemented with active muscle but without any activation; case 2: HBM on which no active muscle at all was implemented; case 3: HBM implemented with active muscle and activation from the experiment were input. Excursions of head top, head CG, T1 and T12 are shown in **Figure 6-1-1** and **Figure 6-1-2**. As excursions in this validation were curves of x-displacement versus z-displacement and no time-domain displacements were provided in the literature, the similarity of them could not be analyzed by time domain statistical tools such as correlation analysis (CORA). Therefore the peak values of displacements in x and z directions were listed in **Table 6-1-1** to qualitatively compare simulations and the experiment.

Figure 6-1-1 is the validation of V4.5. It can be observed from the figure that the trends of excursions of 5 cases are similar to the volunteers from the experimental literature: The head top and head CG of both models and volunteers first moved forward and downward, and then bounced backward and upward; the T1 and T12, on the other hand, moved forward and upward first and bounced backward and downward (before-after excursion models for T1 and T12 overlapped with each other).

Without muscle and no activation cases were set up as a baseline. Because passive soft tissue properties were not considered in this study, these two cases were also to confirm that PE was not activated. It can be clearly observed from both the **Figure 6-1-1** and the **Table 6-1-1** that all four excursions of these two cases overlapped with each other, which verified that the passive soft tissue properties of Hill-type muscle were not considered in this study. Besides, based on the figure and the table, the no activation and without muscle cases had the highest displacement along x and z axes, and the trend of excursions was the closest to the volunteers. In the relaxed original case (case 3), the superficial muscles that were measured in the experiment used the exact same activation curves as measured. Other superficial muscles and all deep muscles which were not measured in the experiment used activation level curves as the muscles close to them and measured in the experiment. However, as shown in the **Figure 6-1-1**, **Figure 6-1-2** and the **Table 6-1-1**, the peak x and z displacements of both Version 4.5 and Version 5.0 model were much less as compared to the volunteers. This indicated that the activation levels of unmeasured muscles in case 3 might not be close to their real activation levels in the experiment. Since another literature suggested that in a static relaxed sitting position, which was similar to the position of volunteers in the experiment, the activation levels of deep trunk extensors were about 50% that of superficial trunk extensors, whereas the activation levels of deep trunk flexors were about 150% that of superficial trunk flexors. Therefore in case 4, activation levels of all superficial trunk muscles were kept the same as case 3, whereas activation levels of all deep trunk extensors and deep trunk flexors were adjusted to 50% and 150% that of case 3, respectively. The same

assumption was made for neck muscles. Deep neck muscles were also adjusted to be the same as trunk muscles in case 4. Case 5 did not activate deep muscles at all as their activations were not provided by the experiment. By observing these two cases, it can be found from both the figure and the table that the models in these two cases moved much more forward than case 3, and excursions were closer to the experiment.

From both the **Figure 6-1-2** and the **Table 6-1-1**, it can be concluded for validation of V4.5 that: The excursions of the original relaxed case were the least similar to the experiment; followed by the excursions of the relaxed adjusted case and the relaxed superficial only case; the excursions of no activation and without muscle cases overlapped with each other and were the most similar to the experiment.

For V5.0, a similar trend of the 5 cases as compared to V4.5 was observed on **Figure 6-1-2** and **Table 6-1-1**. The relaxed original case had the lowest excursions, following the relaxed adjusted and the relaxed superficial only cases. Excursions of no activation and without muscle cases overlapped each other and had the most excursion, excursions of head top and head CG were even more than the experiment. It is observed from both the shape of excursions and the max displacements that except the baseline cases (no activation and without muscle), case 5 (relaxed superficial only) gives the best excursions compared with the experiment.

By comparing excursions of V4.5 and V5.0, it had shown that in each case, V5.0 always moved more forward and downward than V4.5, and the excursions of V5.0 more resembles the experiment than the V4.5. Based on peak x- and z-displacements of V4.5 and V5.0, it was also observed that in every case, peak x-displacements of V5.0 were

always more than V4.5, whereas peak z-displacements of V5.0 were always less than V4.5.

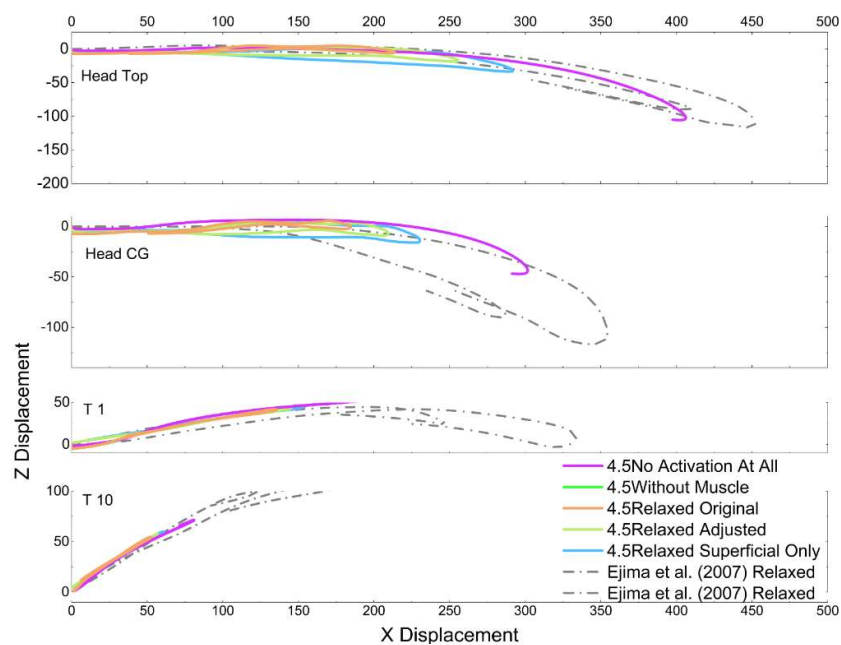


Figure 6-1-1: Results of the validation (V4.5)

Note: Excursions of no activation at all and without muscle cases almost overlapped each other

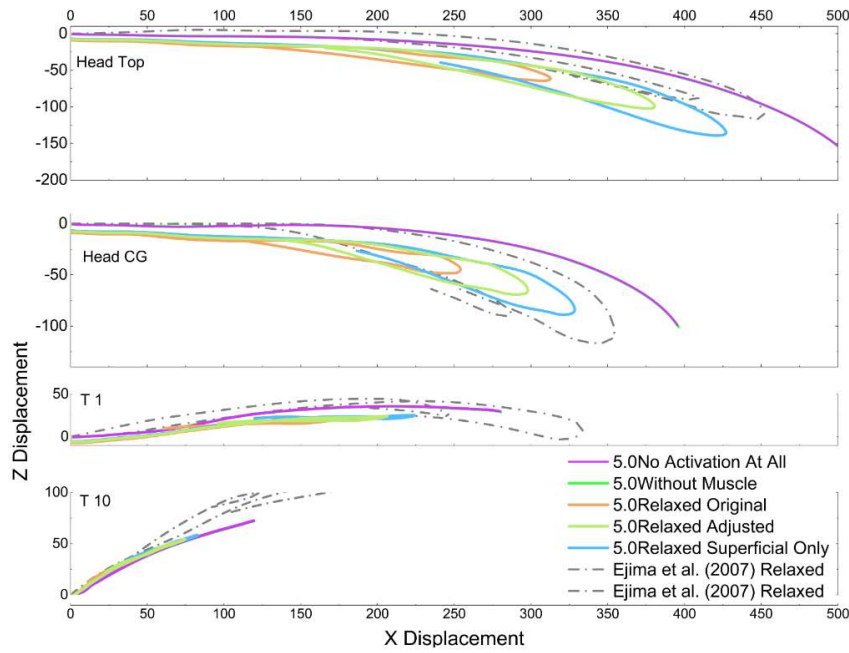


Figure 6-1-2: Results of the validation (V5.0)

Note. Excursions of no activation at all and without muscle cases almost overlapped each other

Table 6-1-1: Peak displacement along x and z axis between HBM and 2 subjects in Ejima et al (2007)

	Case	Head top x	Head top z	Head CG x	Head CG z	T1 x	T1 z	T10 x	T10 z
Exp	Vol 1	455.1	-121.7	359.0	-121.4	336.5	43.1	186.9	112.2
	Vol 2	417.9	-91.6	292.0	-91.6	253.2	44.8	131.3	82.4
V4.5	1	406.1	-105.7	301.7	-47.1	195.8	53.9	80.9	71.3
	2	406.1	-105.7	301.7	-47.1	195.8	53.9	80.9	71.3
	3	213.7	-7.3	184.7	-7.3	135.4	41.9	51.9	54.5
	4	255.6	-18.8	209.3	-8.9	145.3	43.6	56.9	57.5
	5	291.8	-33.6	230.4	-15.9	154.2	45.4	60.9	59.9
V5.0	1	508.1	-168.6	395.3	-99.0	279.7	35.9	119.3	72.5
	2	508.1	-168.6	395.3	-99.0	279.7	35.9	119.3	72.5
	3	312.6	-64.3	254.0	-48.5	182.9	23.4	63.0	48.4
	4	380.6	-102.2	298.0	-66.9	205.9	24.2	74.4	54.3
	5	427.0	-139.3	328.5	-88.9	224.0	25.4	82.6	58.2

Note. Vol 1: volunteer 1 in the experiment; Vol 2: volunteer 2 in the experiment; 1: case 1 no activation at all; 2: case 2 without muscle; 3: case 3 relaxed original; 4: case 4 relaxed adjusted; 5: case 5 relaxed superficial only

6.2 Results of the High-speed Frontal Crash

This section shows the results of the high-speed frontal crash. For V4.5 and V5.0, forces on L1, L3, and L5 of 8 cases including muscles fully activated at 0ms, 40ms, and 80ms; half activated at 0ms, 40ms, and 80ms; and two baseline cases of without muscle and no activation are represented in **Figure 6-2-1** and specific numbers are in **Table 6-2-1**. The timings of peak muscle forces were also collected and shown in **Figure 6-2-3** and **Table 6-2-2**.

In general, it can be observed from the figure that in each case lumbar force decreases from L5 to L1. For the same vertebral level of V4.5, forces of no activation and without muscle were almost equal. And when the activation timing was the same, the force of the fully activated case was always higher than half activated case. It can be observed that for all fully activated cases in V4.5, lumbar force on each vertebral level decreased with the timing of activation. Supplemented by **Table 6-1-1**, it has also been demonstrated that on each vertebral level, the fully activated at 80ms case always has lower force than the other two cases. For half activated cases by observing both the figure and the table, the forces of 0ms and 40ms cases were still higher than 80ms case. However, the half activated at 40ms case has slightly higher force than 0ms case on each vertebra, which was opposite to the fully activated cases.

The similar trend was observed for V5.0. From both **Figure 6-2-1** and the **Table 6-2-1**, it was shown that the no activation case has almost the same force on each vertebral level. On each vertebra, the force increased with activation level, and decreased with the timing of activation. **Figure 6-2-2** also showed that when muscles were contracting, the spine tension was less or eliminated than the no activation and without muscles cases. And from both the figure and the table, it was shown that for every vertebra in fully activated cases and L5 of half activated cases, simulations of activated at 80ms have significantly lower forces than other simulations.

It was also observed that when other parameters were kept constant, V5.0 always has higher force than V4.5, except for L3 and L5 in fully activated cases. For the forces on L3 and L5 of fully activated cases, V4.5 sustained relatively higher forces than V5.0. V5.0 was always more compressed than V4.5 as an example of the geometry of the without muscle models at 100ms shown in **Figure 6-2-4**.

The timing of peak force was also compared. It can be found that in general except some conditions of L5, most timings of peak lumbar force appear between 80-100ms.

For V4.5, when other parameters are the same, the fully activated model always reaches the peak force earlier than the half-activated model, but no clear trend was observed for no activation and without muscle models. In each case, the timing of peak force decreases from L1 to L5, except for the fully activated at 80ms. The timing of peak force increases with the timing of activation except for the half activated on L1. The timing of peak force on L1 of the half-activated model at 40ms was earlier than at 0ms.

For V5.0, the timing of peak force on L5 is always earlier than L3 and L1, but the trend between L1 and L3 is not clear. Under certain conditions, L3 reaches peak force earlier, whereas under other conditions L1 reaches peak force earlier. When the activation level is the only variable, the fully activated models reach the peak force earlier than half activated models. The timing of no activation and without muscle simulations are the slowest to reach peak force on L1 and L5. However, on L3 these two cases become the earliest to reach the peak force. When only considering about the timing of activation, for both fully and half activated cases on each vertebral level, the case activated at 80ms always reaches peak force later than at 0ms. However, no clear trend has been shown in cases activated at 40ms.

Between V5.0 and V4.5, it is found that under the same conditions, V5.0 also reaches peak force later for L1 and L3; however for L5, V5.0 reaches peak force earlier.

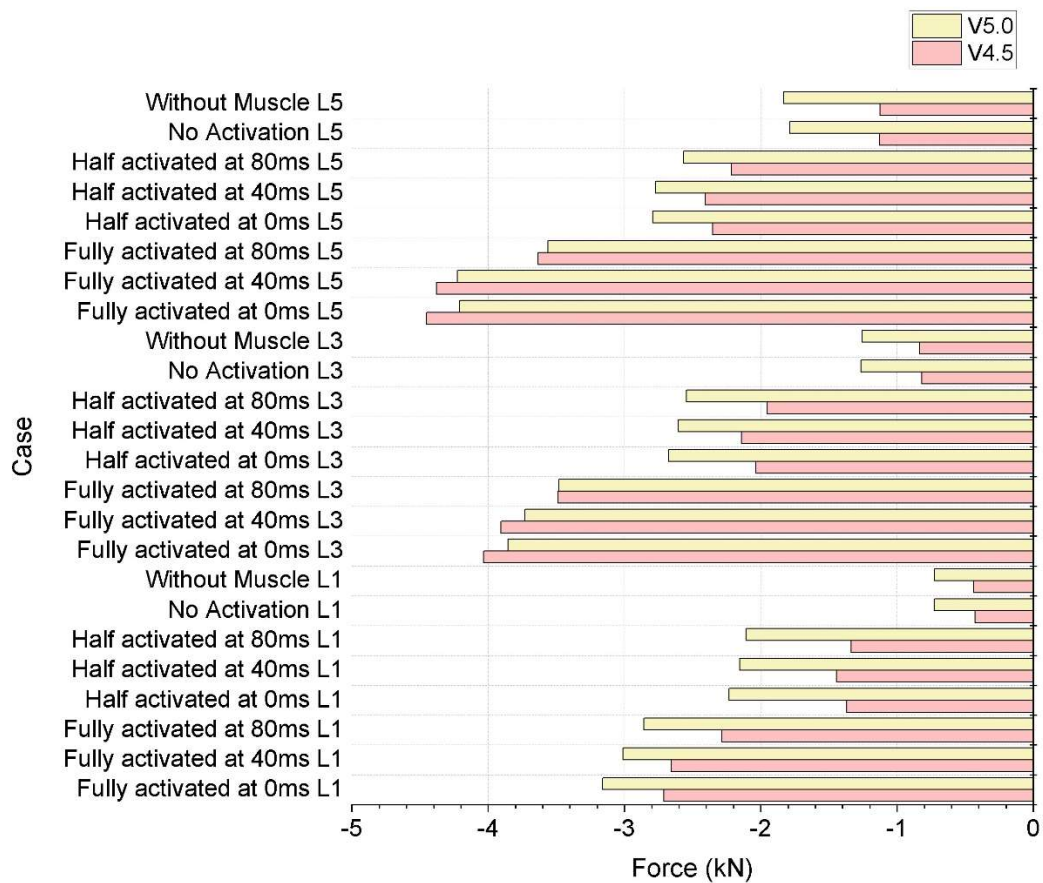


Figure 6-2-1: Peak compressive lumbar forces (kN)

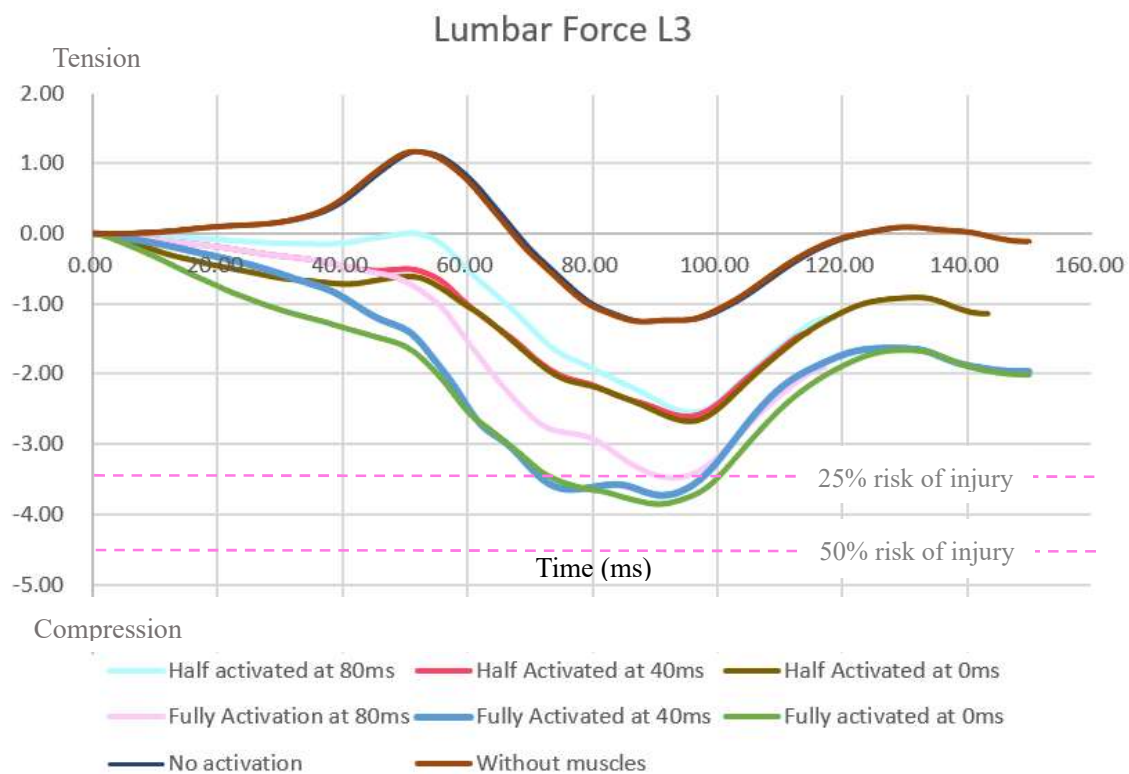


Figure 6-2-2: An example of force trace: V5.0 on L3

Note: The pink-dot lines represent 25% and 50% risk of injury based on the force-injury risk relationship curve from Stemper et al., (2018)

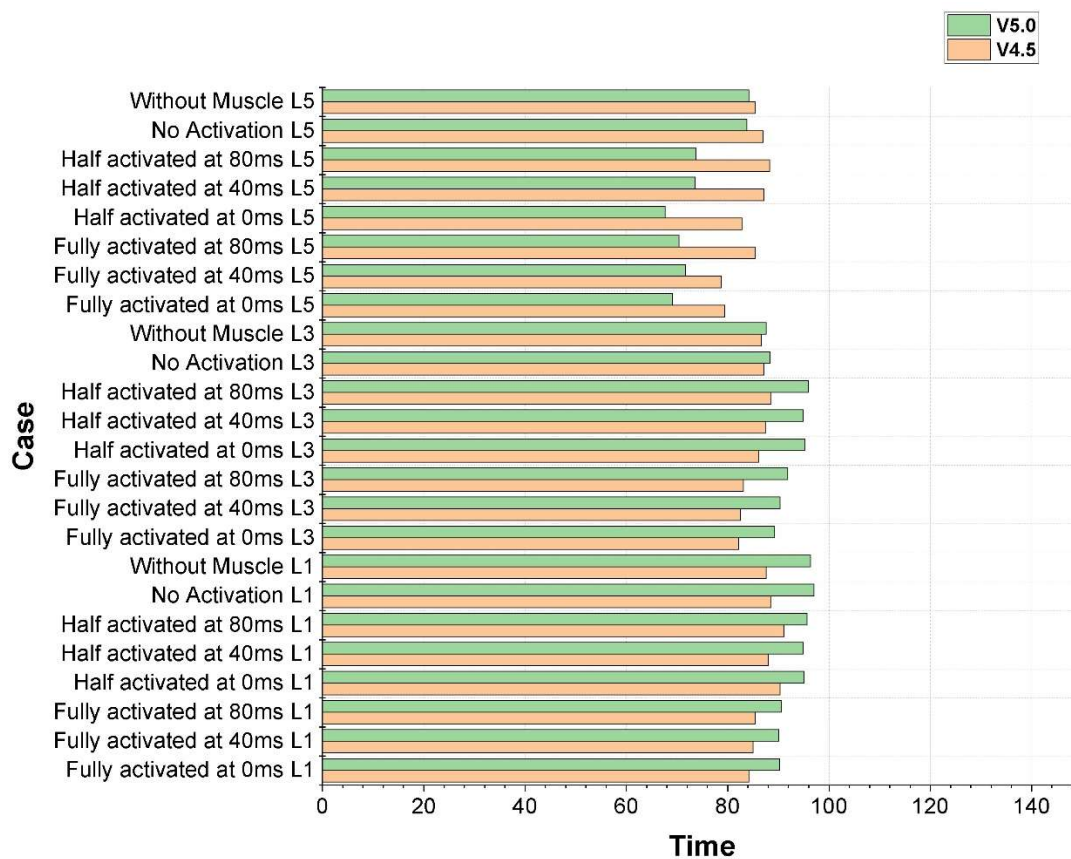


Figure 6-2-3: Timing of peak compressive force (ms)

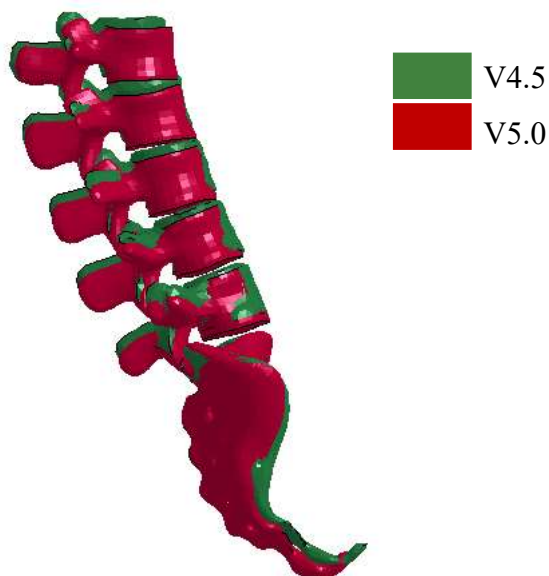


Figure 6-2-4: Lumbosacral spine geometry for the without muscle case at 100ms

Table 6-2-1: Peak compressive lumbar force (kN)

Version	Case	L1	L3	L5
V4.5	Fully activated at 0ms	-2.7112	-4.03272	-4.4547
	Fully activated at 40ms	-2.65641	-3.9073	-4.3784
	Fully activated at 80ms	-2.284	-3.4849	-3.63318
	Half activated at 0ms	-1.36834	-2.03756	-2.35251
	Half activated at 40ms	-1.44268	-2.14077	-2.40928
	Half activated at 80ms	-1.33648	-1.95088	-2.21466
	No activation	-0.42696	-0.81729	-1.12654
	Without muscles	-0.43641	-0.83554	-1.12415
V5.0	Fully activated at 0ms	-3.16193	-3.8545	-4.20833
	Fully activated at 40ms	-3.01005	-3.73006	-4.22526
	Fully activated at 80ms	-2.85764	-3.48075	-3.55999
	Half activated at 0ms	-2.23132	-2.67542	-2.79215
	Half activated at 40ms	-2.15474	-2.60542	-2.77133
	Half activated at 80ms	-2.10841	-2.54531	-2.56634
	No activation	-0.72759	-1.26341	-1.7849
	Without muscles	-0.72267	-1.25606	-1.83146

Table 6-2-2: Timing of peak compressive force (ms)

Version	Case	L1	L3	L5
V4.5	Fully activated at 0ms	84.2	82.2	79.4
	Fully activated at 40ms	85.0	82.5	78.7
	Fully activated at 80ms	85.5	83.1	85.4

Version	Case	L1	L3	L5
	80ms			
	Half activated at 0ms	90.4	86.1	82.8
	Half activated at 40ms	88.1	87.5	87.2
	Half activated at 80ms	91.1	88.6	88.3
	No activation	88.6	87.2	87.0
	Without muscles	87.6	86.6	85.4
V5.0	Fully activated at 0ms	90.3	89.3	69.1
	Fully activated at 40ms	90.1	90.4	71.7
	Fully activated at 80ms	90.7	91.9	70.4
	Half activated at 0ms	95.1	95.3	67.7
	Half activated at 40ms	94.9	94.9	73.6
	Half activated at 80ms	95.9	95.7	73.8
	No activation	97.1	88.4	83.8
	Without muscles	96.4	87.6	84.2

VII. DISCUSSION

This study aimed to investigate the effect of muscle activation and the timing of activation of the lumbar musculature on kinematic responses of occupants during a high-speed frontal central crash. Two versions (V4.5 and V5.0) of the GHBMC HBM M50 were used in this study.

7.1 Validation

The study validated the GHBMC HBM implemented with lumbar musculature. Five cases including no activation, without muscle, relaxed original, relaxed adjusted, and relaxed with only superficial muscles activated were constructed for each version. For each version, excursions of no activation and without muscle overlapped with each other. Excursions of head top, head CG, T1 and T10 relative to the pelvis were compared with the experiment in the literature.

It is observed for each version that excursions of no activation and without muscle cases overlapped with each other. This confirmed that the passive soft tissue properties were not simulated in the model. This is because if a Hill-type muscle does not have passive soft tissue properties and not activated at the same time, it does not generate any force. Therefore, the model with non-activated muscle should have almost the same kinematic and kinetic responses as the model without active muscles.

It is also observed that for V5.0, the relaxed-original case has the least excursions, followed by the relaxed adjusted case and the relaxed superficial only case. The no activation and without muscle cases have the highest excursions. This trend is easy to

explain from the perspective of muscle functions and activation levels. The function of muscles is to control body movement. The Hill-type muscles control body movements by generating forces at the origins and insertions of muscles. In this specific study, active muscles restrain the movement of the spine, or make the spine less “flexible”. This is why the no activation and without muscle cases have the highest excursion. In these two cases, the movement of the spine was not constrained by active muscles at all.

Comparing the other two cases to the relaxed original case, the relaxed adjusted case had less activation levels of deep extensors and more activation levels of deep flexors.

Therefore, the spine in this case was expected to bend more forward. This is why the model in the relaxed adjusted case moved more forward than the relaxed original case.

For the relaxed superficial only case, as all deep muscles were not activated, the model in this case has less muscle activations in general than the relaxed original and relaxed adjusted case. Similar as the no activation and without muscle cases, the model in this case was less constrained by active muscles, therefore they had higher excursions than the relaxed original and relaxed adjusted cases.

By comparing these 5 cases for each version, two things can be concluded: 1) Since the relaxed adjusted case adjusted activation levels of deep muscles as suggested by another literature, and its excursions were indeed more similar to the experiment, it indicates that although deep muscle activations were not provided from experimental data, perhaps their activation levels were close to what was set in the relaxed adjusted case; 2) The relaxed superficial only, no activation and without muscle cases had less muscle activations in general, which indicated that muscle activations reported in the

experiment might be higher than reality. It is possible as these muscle activation level curves in a relaxed condition were obtained by normalizing (dividing) values of relaxed EMG curves by the maximum value of EMG curves when volunteers were in a tensed situation, and it is not clear from the literature if these maximum values were the same as the maximum voluntary isometric contraction (MVIC) of the muscle. For example, by measuring the MVIC of erector spinae, a volunteer is asked to lift the head, shoulders and elbows with hands on the neck in a prone position (Dankaert et al., 2004), whereas in the experiment, the volunteers were measured in a sitting position.

Comparing excursions of V4.5 and V5.0, it is observed that for each case, V5.0 always moves more forward and downward than V4.5. One potential reason is that the material properties of lumbar region of V4.5 and V5.0 are different. The major differences in the lumbar region between these two versions were: 1) the lumbar spine of V4.5 was rigid as opposed to the deformable of V5.0; 2) The intervertebral discs of V4.5 were constructed by beam elements whereas in V5.0, they had the shape of a real human spine and were deformable as well. These differences may lead to the lumbar spine of V5.0 being easier to bend whereas V4.5 was stiffer, so V5.0 naturally moved more forward and downward. When in the same condition, excursions of V5.0 were more similar to the experiment; it is possible that V5.0 is more capable to predict human kinematic responses during an impact as opposed to V4.5.

The better predictability of human kinematic and kinetic response of deformable spine and detailed intervertebral discs has been confirmed by literature. Aira et al. (2019) compared kinematic and kinetic responses of GHBM HBM M50 V4.5 which had rigid

thoracic spine and an updated model with deformable thoracic vertebrae and intervertebral disc similar to the reality under a rear pendulum impact and a lateral shoulder impact with experimental results. Results showed that the updated model had a better biofidelity than the V4.5. Somasundaram et al. (2019) replaced rigid thoracolumbar vertebrae of the GHBMCM50 by deformable vertebrae and changed intervertebral discs to be closer to the experiments. Their study investigated spinal acceleration of two models. Similar results showed that the updated model had better biofidelity.

There are still some differences between excursions of V5.0 and the experiment. This may be because that although some muscle activation inputs were based on the reasonable assumption as no information were provided by the literature, they might still deviate from reality. Moreover, the difference of positions between the GHBMCM50 and the experiment might also lead to divergence. Finally, the GHBMCM50 represents an average geometry of a 26-year-old male, which might also result into difference of excursions between V5.0 and the experiment.

In general, V5.0 better predicts human kinematic responses during an impact. Although the results of validation of V5.0 is still different from the experiment, it may mainly be because the limited information of muscle activations and geometry difference between the GHBMCM50 and volunteers in the experiment

7.2 Investigation of the Effect of the Musculature in the High-speed Frontal Crash

After the validation, in order to investigate the effects of the lumbar musculature on kinematic responses of occupants during the high-speed frontal central crash, 16

simulations were set up and each version had 8 simulations. These 8 simulations were: full activation at 0ms, 40ms, and 80ms; half activation at 0ms, 40ms, and 80ms; no activation and without muscles. Lumbar spine forces at L1, L3, and L5 were collected for further investigating the effects of lumbar musculature.

It was observed that the peak compressive lumbar force increased from L1 to L5, which is consistent with previous literature. Patel in 2011 observed from an HBM study that during body movements such as standing normally, weightlifting, and squatting, the intervertebral disc force at L1 was always the lowest and highest at L5. Ye et al (2018) reconstructed 11 cases of real-world frontal crashes. They found that the compressive force generally increased from L1 to L4. This seems different from what was reported in the previous articles that L1 had more chance of fracture in the frontal crash (Ching et al., 2013; Jakobsson et al., 2016). However, it is still reasonable because the cross-sectional area and the thickness of L1 are smaller than the other vertebrae. Although L1 has the lowest force, its relatively smaller size could impose a high chance of injuries.

By comparing the groups implemented among no activated muscles, half activated muscles and fully activated muscles, it is shown that the lumbar spine force increased with the muscle activation level. And the muscle contraction reduced or eliminated the spine tension. This is reasonable as muscles with higher activation levels generate more force. The effect of muscle contraction on bony injuries has been reported by many studies. To investigate the relationship between the muscle activation of lower extremities muscles and the impact force, Pithioux et al. (2005) asked volunteers to generate 25%, 50% and 75% of lower extremities muscle forces from the beginning to

the end of sled tests. Results showed that the impact force between foot and foot pedal was proportional to the muscle activation. Tencer et al (2002) reported that in a frontal crash, leg muscle contraction might generate more force than no activation which might contribute to femur fracture. Nie et al (2018) also observed that the muscle activation of lower extremities in vehicle crashes increases axial forces of the femur and tibia. Fewer studies have focused on the lumbar muscle contraction in vehicle crash, but it was reported in seizure whereby the patients would uncontrollably tense their muscles. Such lumbar muscle contraction was strong enough to induce lumbar vertebral fracture, especially for young males who have strong musculature (Sharma et al., 2011). Therefore, the lumbar muscle contraction can induce a risk of lumbar spine fractures.

In addition to the muscle activation level, the timing of the activation also affected the risk of lumbar spine injuries. The results of this study revealed that the lumbar force decreased with the timing of the activation. The effect of activation timing was reported by many in the literature. Eckner et al. (2014) observed that anticipatory neck muscle activation reduced head kinematic responses of volunteers. Jin et al (2017) also observed that the timing of neck muscle contraction affected the risk of head injuries. Although there are few pieces of literature focused on the timing of lumbar muscle activation, it has been confirmed that the timing of muscle activation can affect kinematic responses of subjects during an impact.

It was also observed the lumbar force was significantly lower when activated at 80ms than at 0ms and 40ms, especially in the fully activated group. One of the potential reasons can be that the effect of timing of activation may be associated with the timing of

peak deceleration of the vehicle. It was found from the deceleration pulse used in this study that the first peak deceleration occurred at 30-35ms and the second was around 45-50ms. 0ms was before occurrences of peak accelerations, 80ms was after occurrences while 40ms was in between. Perhaps for the group activated at 80ms, the bracing was too late to reduce the effect of fast deceleration. The effect of the acceleration pulse may also be the reason why for some vertebra level in some groups, the force when muscles reach a peak activation level at 40ms is slightly higher than at 0ms.

By comparing forces at the same vertebral level under the same condition, it was observed that V5.0 generally predicts higher force than V4.5. In the observation of models of V5.0 and V4.5, it was found that the lumbar spine in V5.0 was always more compressed, perhaps potentially exposing the lumbar spine in V5.0 to more forces. For L3 and L5 in the fully activated group, although not very significant, V4.5 sustained higher force than V5.0. This was probably due to the difference between material properties in the lumbar region. For example, when the displacement is high, the rate of force-displacement on intervertebral discs in V4.5 increases as well. It can also be due to the different effect of adjacent soft tissue because of their different geometry. But in general, given the same scenario, lumbar spine of V5.0 did sustain higher forces than V4.5.

It was found that the timing of peak lumbar force was all after 65ms, which is after the peak acceleration of the vehicle. L5 reaches peak force earlier than L1 and L3. This may be because as Nordhoff (2005) described, in frontal crash occupants reach their peak acceleration after the vehicle reaches its maximum acceleration. Therefore, the

timing of peak lumbar force may also be delayed. Since the L5 is close to the hip region which is constrained to the vehicle by a seatbelt, its timing of peak force can be linked to the timing of peak acceleration of the vehicle. Therefore, L5 sustains peak force earlier than L1 and L3. It is also found that the V4.5 reaches peak lumbar force earlier than the V5.0 except for L5. This can also be because the influence of differences between lumbar spines of V4.5 and V5.0. There are some variations or trends of peak force timing among cases of various activation level and timing of activation. However, as these variations and trends are not as clear as of the peak lumbar force, and most of timings are within 80-100ms seconds, the muscle activation level and the timing of activation may not affect the timing of peak force much.

Last but not least, it is also observed from this study that the HBM implemented with lumbar muscles may give a better prediction of the risk of lumbar spine injuries. It has been discussed in previous sections that the lumbar spine has a risk of injuries during frontal central crashes (Scullion et al., 2011; Pintar et al., 2012). Stemper et al. (2018) investigated the relationship between the lumbar spine force and the risk of injuries by compressing intact human lumbar spines under injurious loadings. The occurrence rates of specific types of lumbar spine fracture such as the burst fracture and the wedge fracture among all fractures were similar to what was reported in the real world during frontal crashes by Pintar et al. (2012). Therefore, this curve can be used to predict the risk of lumbar spine injuries in real frontal crashes. Referencing to the relationship between lumbar spine force and the risk of injury reported by Stemper et al. (2018) (**Figure 7-2-1**), it was observed from this study that the models implemented with

activated muscles had a higher risk of fracture. Taking an example of V5.0 without muscle and fully activated at 0ms cases as shown in **Figure 7-2-1**, the risk of lumbar spine injury of the without muscle case was below 10%, whereas the risk of the fully activated case was around 40% and can be as high as 60%. Figure 6-2-2 also confirmed that the fully activated models had higher risk of injury on L3 than the model without muscles. Meijer et al. (2012) also observed that the HBM with active neck muscle better predicted kinematic responses of volunteers. It should be noticed that the figure by Stemper et al (2018) in turn also proved that lumbar muscle contraction, especially anticipatory muscle contraction, could result in a higher chance of lumbar spine injuries in a vehicle crash, as discussed in the previous paragraphs.

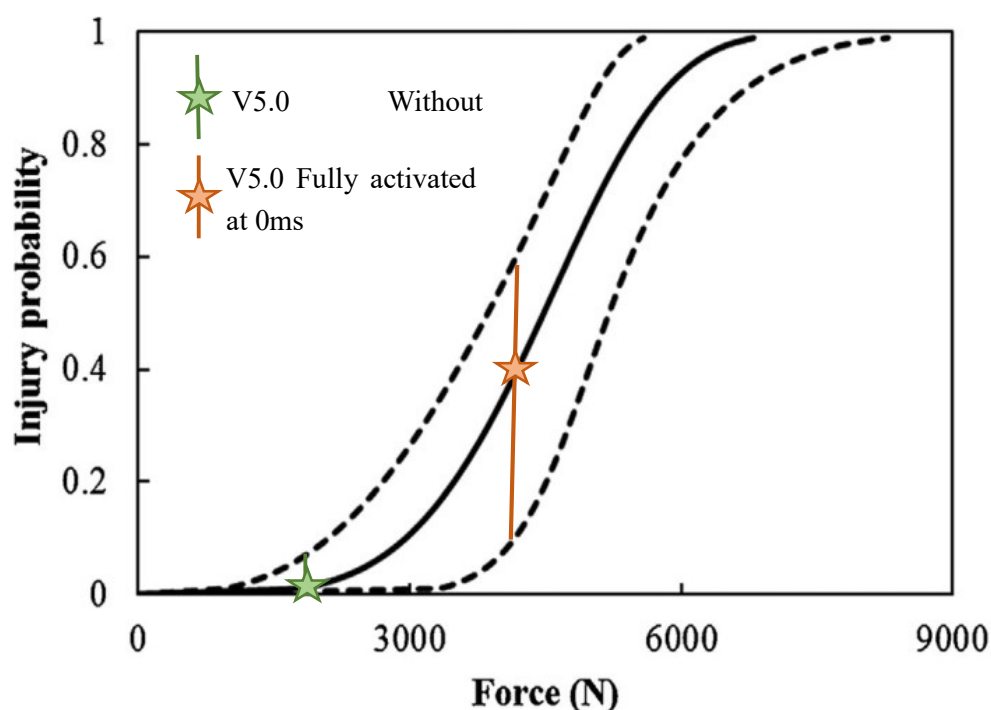


Figure 7-2-1: The relationship of the risk of the injury and the lumbar spine force (Adapted from Stemper et al., 2018)

In general, this study observed that activation level and timing of activation of trunk musculature has an effect on the risk of lumbar spine injuries during the frontal central crash. Powerful anticipatory muscle contraction is related to higher risk of injury. As it is impossible to train every occupant to avoid early bracing muscles during a high-speed instantaneous crash, vehicle safety systems may need to be improved to protect occupants from lumbar spine injuries during a crash.

VIII. CONCLUSION

It has been determined from the literature that the lumbar spine has a higher risk of injuries in the frontal crash and the incidence of lumbar spine injuries during frontal crashes has been increasing as a function of vehicle model year. Because the mechanism of the lumbar musculature in a frontal crash has not been fully understood, this study aimed to investigate the effect of the lumbar musculature on the kinematics of occupants in a high-speed frontal crash. It was observed that powerful bracing and early realization of the upcoming impact were associated with a higher risk of lumbar spine injuries. As it is impossible to train every occupant to avoid bracing lumbar muscles before a vehicle crash, this study suggested that it is necessary for the safety system to be improved to protect the lumbar region of vehicle occupants in a frontal crash.

IX. LIMITATIONS AND FUTURE DIRECTION

As mentioned previously in the validation, V4.5 had lower excursions than V5.0, and less activation associated with higher excursions. It suggests that in the future, perhaps applying muscle activations less than ordinary on the GHBM HBM V4.5 may give a better trajectory.

Similar to other studies, this study also has limitations. The validation was only applied in a low-speed crash environment. Currently, it is not possible to measure muscle activations of human subjects in high-speed crash tests. However, driver simulator tests have the potential to obtain muscle activations without ethical concerns. The driver simulator can virtually replicate high-speed crash scenarios so that kinematic responses and muscle activations of occupants in these scenarios can be measured (Hault-Dubrulle et al., 2010; Gao et al., 2015). In future studies, driver simulators may help validate HBM muscle activation with better precision.

It was noticed that in some cases half activated at 40ms had slightly higher forces than the half 0ms. But since the difference was less than 5%, it was not significant. However, because the 40ms was close to the timing of the peak deceleration, perhaps in some cases if bracing at the time of the impact, it can lead to an even higher risk of injury. Future studies can set up more simulations to investigate how the timing of bracing affects the kinematics of occupants.

Only one deceleration pulse was used in this study, therefore the effect of deceleration pulses might be ignored. Further studies can replicate the same method of this study but applying different deceleration pulses to the vehicle to investigate the effect

of deceleration pulse. If results are still consistent with the current study, it will be with more confidence to conclude that the muscle activation and the timing of the activation do affect kinematic responses of occupants in the frontal crash.

The HBM used in the current study represented a young male human. However, it was also found from the literature that the vehicle crash was one of the leading reasons for injuries and fatality of children (Seacrist et al., 2014). Therefore, using child models representing children in future vehicle crash studies may help improve protections of children in vehicles.

BIBLIOGRAPHY

- Adolph, T., Ott, J., Eichhoff, B., & Johannsen, H. (2015). *What is the Benefit of the Frontal Mobile Barrier Test Procedure?* 1–11.
- Adolph, T., Wisch, M., Eggers, A., Johannsen, H., Cuerden, R., Carroll, J., ... Sander, U. (2013). *Irc-13-17 2013*. 91–102.
- Aira, J., Guleyupoglu, B., Jones, D., Koya, B., Davis, M., & Gayzik, F. S. (2019). Validated thoracic vertebrae and costovertebral joints increase biofidelity of a human body model in hub impacts. *Traffic injury prevention, 20*(sup2), S1–S6.
<https://doi.org/10.1080/15389588.2019.1638511>
- Arbelaez, R. A., Aylor, D., Nolan, J. M., Braitman, K. A., & Baker, B. C. (2006). Crash modes and injury patterns in real-world narrow object frontal crashes. *International Research Council on the Biomechanics of Impact - 2006 International IRCOBI Conference on the Biomechanics of Impact, Proceedings*, (September), 333–336.
- Astfalck, R. G., O’Sullivan, P. B., Smith, A. J., Straker, L. M., & Burnett, A. F. (2013). Lumbar spine repositioning sense in adolescents with and without non-specific chronic low back pain - An analysis based on sub-classification and spinal regions. *Manual Therapy, 18*(5), 410–417. <https://doi.org/10.1016/j.math.2013.02.005>
- Brinckmann, P., Biggemann, M., & Hilweg, D. (1989). Prediction of the compressive strength of human lumbar vertebrae. *Spine, 14*(6), 606–610.
<https://doi.org/10.1097/00007632-198906000-00012>
- Choi, H. Y., Sah, S. J., & Lee, B. (2005). *Experimental and numerical studies of muscular activations of bracing occupant*. (January 2005), 10. Retrieved from <https://www-nrd.nhtsa.dot.gov/pdf/esv/esv19/05-0139-O.pdf>
- Combest, J. J. (2016). Current Status and Future Plans of the GHBMC (Global Human Body Models Consortium). *Human Modeling and Simulation in Automotive Engineering*, 1–40. Retrieved from http://www.ghbmc.com/wp-content/uploads/2016/10/HuMo16_15_Combest_GHBMC.pdf
- Dankaerts, W., O’Sullivan, P. B., Burnett, A. F., Straker, L. M., & Danneels, L. A. (2004). Reliability of EMG measurements for trunk muscles during maximal and sub-maximal voluntary isometric contractions in healthy controls and CLBP patients. *Journal of Electromyography and Kinesiology, 14*(3), 333–342.
<https://doi.org/10.1016/j.jelekin.2003.07.001>
- Doud, A. N., Weaver, A. A., Talton, J. W., Barnard, R. T., Meredith, J. W., Stitzel, J. D., ... Miller, A. N. (2015). Has the Incidence of Thoracolumbar Spine Injuries Increased in the United States From 1998 to 2011? *Clinical Orthopaedics and Related Research, 473*(1), 297–304. <https://doi.org/10.1007/s11999-014-3870-9>

- Ejima, S., Ono, K., Holcombe, S., Kaneoka, K., & Fukushima, M. (2007). A study on occupant kinematics behaviour and muscle activities during pre-impact braking based on volunteer tests. *International Research Council on the Biomechanics of Injury - 2007 International IRCOBI Conference on the Biomechanics of Injury, Proceedings*, pp. 31–45.
- Eurostat. (2017). Statistical pocketbook 2017. In *Publications Office of the European Union, 2017* (Vol. 31). <https://doi.org/10.2832/147440>
- Fish, J., & Belytschko, T. (2007). *A First Course in Finite Elements* (J. Fish & T. Belytschko, Eds.). Wiley, 2007.
- Forman, J. L., Lopez-Valdes, F. J., Duprey, S., Bose, D., Del Pozo De Dios, E., Subit, D., ... Segui-Gomez, M. (2015). The tolerance of the human body to automobile collision impact - A systematic review of injury biomechanics research, 1990-2009. *Accident Analysis and Prevention*, *80*(2015), 7–17. <https://doi.org/10.1016/j.aap.2015.03.004>
- Gao, Z., Li, C., Hu, H., Zhao, H., Chen, C., & Yu, H. (2015). Experimal study of young male drivers' responses to vehicle collision using EMG of lower extremity. *Bio-Medical Materials and Engineering*, *26*, S563–S573. <https://doi.org/10.3233/BME-151347>
- Gayzik, F. S., Moreno, D. P., Vavalle, N. A., Rhyne, A. C., & Stitzel, J. D. (2012). Development of a Full Human Body Finite Element Model for Blunt Injury Prediction Utilizing a Multi-Modality Medical Imaging Protocol. *12th Int'l LS-DYNA User Conf*, (January).
- Hault-Dubrulle, A., Robache, F., Drazétić, P., & Morvan, H. (2009). Pre-Crash Phase Analysis Using a Driving Simulator . Influence of Atypical Position on Injuries and Airbag Adaptation . *The 21st International Technical Conference on the Enhanced Safety of Vehicles Conference (ESV)*, 1–13.
- Highway Traffic Safety Administration, N., & Department of Transportation, U. (2013). *Traffic Safety Facts 2013 Data Key Findings People Killed and Injured, and Fatality and Injury Rates*. (July), 1–12. Retrieved from <https://crashstats.nhtsa.dot.gov/Api/Public/ViewPublication/812169>
- Hong, S. W., Park, C. K., Mohan, P., Morgan, R. M., Kan, C. D., Lee, K., ... Bae, H. (2008). Comparative analysis of a vehicle impacting a rigid barrier, An offset deformable barrier, and a rigid pole. *International Research Council on the Biomechanics of Injury - 2008 International IRCOBI Conference on the Biomechanics of Injury, Proceedings*, (September 2008), 417–420.
- Hu, J., Zhang, K., Reed, M. P., Wang, J. T., Neal, M., & Lin, C. H. (2019). Frontal crash simulations using parametric human models representing a diverse population. *Traffic Injury Prevention*, *20*(sup1), S97–S105. <https://doi.org/10.1080/15389588.2019.1581926>

- Huang, Y., King, A. I., & Cavanaugh, J. M. (1994). Finite element modeling of gross motion of human cadavers in side impact. *SAE Technical Papers*, 103(1994), 1604–1622. <https://doi.org/10.4271/942207>
- Jakobsson, L., Björklund, M., & Westerlund, A. (2016). *IRC-16-22 IRCOBI Conference 2016*. 101–112.
- Jaramillo, H. E., Gómez, L., & García, J. J. (2015). A finite element model of the L4-L5-S1 human spine segment including the heterogeneity and anisotropy of the discs. *Acta of Bioengineering and Biomechanics*, 17(2), 15–24. <https://doi.org/10.5277/ABB-00046-2014-02>
- Jin, X., Feng, Z., Mika, V., Li, H., Viano, D. C., & Yang, K. H. (2017). The Role of Neck Muscle Activities on the Risk of Mild Traumatic Brain Injury in American Football. *Journal of Biomechanical Engineering*, 139(10). <https://doi.org/10.1115/1.4037399>
- Kaufman, R. P., Ching, R. P., Willis, M. M., Mack, C. D., Gross, J. A., & Bulger, E. M. (2013). Burst fractures of the lumbar spine in frontal crashes. *Accident Analysis and Prevention*, 59, 153–163. <https://doi.org/10.1016/j.aap.2013.05.023>
- Kullgren, A., Krafft, M., Nygren, Å., & Tingvall, C. (2000). Neck injuries in frontal impacts: Influence of crash pulse characteristics on injury risk. *Accident Analysis and Prevention*, 32(2), 197–205. [https://doi.org/10.1016/S0001-4575\(99\)00096-2](https://doi.org/10.1016/S0001-4575(99)00096-2)
- Kurutz, M., & Oroszvy, L. (2012). Finite Element Modeling and Simulation of Healthy and Degenerated Human Lumbar Spine. *Finite Element Analysis - From Biomedical Applications to Industrial Developments*, (May 2014). <https://doi.org/10.5772/37384>
- Liu, C., & Subramanian, R. (2020). *The relationship between passenger vehicle occupant injury outcomes and vehicle age or model year in police-reported crashes. Traffic Safety Facts Research Note. Report No. DOT HS 812 937. National Highway Traffic Safety Administration.* (March).
- Lizee, E., Robin, S., Song, E., Bertholon, N., Le Coz, J. Y., Besnault, B., & Lavaste, F. (1998). Development of a 3D finite element model of the human body. *SAE Technical Papers*, 107(1998), 2760–2782. <https://doi.org/10.4271/983152>
- Lorenz, T., Campello, M., Pitman, M. I., & Peterson, L. (2001). Biomechanics of Skeletal Muscle. In M. Nordin & V. H. Frankel (Eds.), *Basic Biomechanics of the Musculoskeletal System* (Third, pp. 148–171). Lippincott Williams & Wilkins.
- Martin, P. G. (2007). *Nhtsa's thor-nt database 2007*. 1–8.
- Marzougui, D., Samaha, R., Nix, L., & Kan, C. (2013). Extended Validation of the Finite Element Model for the 2010 Toyota Yaris Passenger Sedan (MASH 1100kg Vehicle). *Transportation Research Board 92nd Annual Meeting*, (July).
- Morgan, R. M., Cui, C., Digges, K. H., Cao, L., & Kan, C. D. (2012). Impact and injury patterns in between-rails frontal crashes of vehicles with good ratings for frontal crash protection. *Annals of Advances in Automotive Medicine*, 56(January 2009),

255–265.

- Müller, C. W., Otte, D., Decker, S., Stübiger, T., Panzica, M., Krettek, C., & Brand, S. (2014). Vertebral fractures in motor vehicle accidents—a medical and technical analysis of 33,015 injured front-seat occupants. *Accident Analysis and Prevention*, *66*, 15–19. <https://doi.org/10.1016/j.aap.2014.01.003>
- Myklebust, J., Sances, A., Maiman, D., Pintar, F., Chilbert, M., Rauschnig, W., ... Saltzberg, B. (1983). Experimental spinal trauma studies in the human and monkey cadaver. *SAE Technical Papers*. <https://doi.org/10.4271/831614>
- Nachemson, A.L. (1976). The Lumbar Spine An Orthopaedic Challenge. *Spine*, *1*, 59–71.
- National Center for Statistics and Analysis. (2019). *2018 fatal motor vehicle crashes: Overview*. (Traffic Safety Facts Research Note. Report No. DOT HS 812 826). Washington, DC: National Highway Traffic Safety Administration.
- Nie, B., Sathyanarayan, D., Ye, X., Crandall, J. R., & Panzer, M. B. (2018). Active muscle response contributes to increased injury risk of lower extremity in occupant–knee airbag interaction. *Traffic Injury Prevention*, *19*, S76–S82. <https://doi.org/10.1080/15389588.2017.1349898>
- Nordhoff, Lawrence S., J. (2005). Frontal Crashes: Biomechanics and Injuries. In J. Nordhoff, Lawrence S. (Ed.), *Motor Vehicle Collision Injuries: Biomechanics, Diagnosis, and Management* (pp. 427–460). Jones & Bartlett Learning, 2005.
- Nordin, M., Weiner, S. S., & Lindh, M. (2001). Biomechanics of the Lumbar Spine. In M. Nordin & V. H. Frankel (Eds.), *Basic Biomechanics of the Musculoskeletal System* (Third, pp. 256–284). Lippincott Williams & Wilkins.
- Organisation, W. H. (2015). Tables A2 & A10, data from 2013. *Global Status Report on Road Safety 2015*, (ISBN 978 92 4 156506 6), 316–332.
- Östh, J. (2010). Active Muscle Responses in a Finite Element Human Body Model. *Ph.D. Thesis Chalmers University of Technology*.
- Pedram, H., Reza, Z. M., Reza, R. M., Vaccaro, A. R., & Vafa, R. M. (2010). Spinal fractures resulting from traumatic injuries. *Chinese Journal of Traumatology - English Edition*, *13*(1), 3–9. <https://doi.org/10.3760/cma.j.issn.1008-1275.2010.01.001>
- Pintar, F. A., Yoganandan, N., & Maiman, D. J. (2008). Injury mechanisms and severity in narrow offset frontal impacts. *Annals of Advances in Automotive Medicine - 52nd Annual Scientific Conference*, *52*(October), 185–189.
- Pintar, F. A., Yoganandan, N., Maiman, D. J., Scarboro, M., & Rudd, R. W. (2012). Thoracolumbar spine fractures in frontal impact crashes. *Annals of Advances in Automotive Medicine*, *56*, 277–283.
- Rao, R. D., Berry, C. A., Yoganandan, N., & Agarwal, A. (2014). Occupant and crash characteristics in thoracic and lumbar spine injuries resulting from motor vehicle

- collisions. *Spine Journal*, 14(10), 2355–2365.
<https://doi.org/10.1016/j.spinee.2014.01.038>
- Richards, D., Carhart, M., Raasch, C., Pierce, J., Steffey, D., & Ostarello, A. (2006). Incidence of thoracic and lumbar spine injuries for restrained occupants in frontal collisions. *Annual Proceedings - Association for the Advancement of Automotive Medicine*, 2006(February 2006), 125–139.
- Roberts, A. K., & Carroll, J. A. (2003). *Dummy Development to evaluate spine injuries*.
- Saladin, K. S., Gan, C. A., & Cushman, H. N. (2010). *Anatomy & physiology : the unity of form and function* (8th ed.; K. S. Saladin, C. A. Gan, & H. N. Cushman, Eds.). McGraw-Hill Education, 2012.
- Scullion, P., Morgan, R. M., Mohan, P., Kan, C. D., Shanks, K., Jin, W., & Tangirala, R. (2010). A reexamination of the small overlap frontal crash. *Annals of Advances in Automotive Medicine / Annual Scientific Conference ... Association for the Advancement of Automotive Medicine. Association for the Advancement of Automotive Medicine. Scientific Conference*, 54, 137–148.
- Sharma, A., Avery, L., & Novelline, R. (2011). Seizure-induced lumbar burst fracture associated with conus medullaris-cauda equina compression. *Diagnostic and Interventional Radiology*, 17(3), 199–204.
<https://doi.org/10.4261/1305-3825.DIR.3638-10.2>
- Siegmund, G. P., Chimich, D. D., & Elkin, B. S. (2014). Role of Muscles in Accidental Injury. In N. Yoganandan, A. M. Nahum, & J. W. Melvin (Eds.), *Accidental Injury: Biomechanics and Prevention* (pp. 611–642). Springer, 2014.
- Somasundaram, K., Zhang, L., Sherman, D., Begeman, P., Lyu, D., & Cavanaugh, J. M. (2019). Evaluating thoracolumbar spine response during simulated underbody blast impact using a total human body finite element model. *Journal of the mechanical behavior of biomedical materials*, 100, 103398.
<https://doi.org/10.1016/j.jmbbm.2019.103398>
- Stemper, Brian D., Pintar, F. A., & Baisden, J. (2014). Lumbar Spine Injury Biomechanics. In N. Yoganandan, A. M. Nahum, & J. W. Melvin (Eds.), *Accidental Injury: Biomechanics and Prevention* (Third, pp. 451–470). Springer, 2014.
- Stemper, Brian D., Chirvi, S., Doan, N., Baisden, J. L., Maiman, D. J., Curry, W. H., ... Shender, B. S. (2018). Biomechanical tolerance of whole lumbar spines in straightened posture subjected to axial acceleration. *Journal of Orthopaedic Research*, 36(6), 1747–1756. <https://doi.org/10.1002/jor.23826>
- Stemper, Brian D., Yoganandan, N., Cusick, J. F., & Pintar, F. A. (2006). Stabilizing effect of precontracted neck musculature in whiplash. *Spine*, 31(20), 733–738.
<https://doi.org/10.1097/01.brs.0000240210.23617.e7>
- Stigson, H., Kullgren, A., & Rosén, E. (2012). Injury risk functions in frontal impacts using data from crash pulse recorders. *Annals of Advances in Automotive Medicine*,

56, 267–276.

- Stilwell, P., Harman, K., Hsu, W., & Seaman, B. (2016). Multiple seizure-induced thoracic vertebral compression fractures: A case report. *Journal of the Canadian Chiropractic Association*, *60*(3), 252–257.
- Tang, L., Zheng, J., & Hu, J. (2020). A numerical investigation of factors affecting lumbar spine injuries in frontal crashes. *Accident Analysis and Prevention*, *136*(December 2019), 105400. <https://doi.org/10.1016/j.aap.2019.105400>
- Tencer, A. F., Kaufman, R., Ryan, K., Grossman, D. C., Henley, M. B., Mann, F., ... Eastman, B. (2002). Femur fractures in relatively low speed frontal crashes: The possible role of muscle forces. *Accident Analysis and Prevention*, *34*(1), 1–11. [https://doi.org/10.1016/S0001-4575\(00\)00097-X](https://doi.org/10.1016/S0001-4575(00)00097-X)
- Wang, M. C., Pintar, F., Yoganandan, N., & Maiman, D. J. (2009). The continued burden of spine fractures after motor vehicle crashes. *Journal of Neurosurgery: Spine*, *10*(2), 86–92. <https://doi.org/10.3171/2008.10.spi08279>
- Ward, S. R., & Lieber, R. L. (2005). Density and hydration of fresh and fixed human skeletal muscle. *Journal of Biomechanics*, *38*(11), 2317–2320. <https://doi.org/10.1016/j.jbiomech.2004.10.001>
- Winters, J. M. (1995). How detailed should muscle models be to understand multi-joint movement coordination? *Human Movement Science*, *14*(4–5), 401–442. [https://doi.org/10.1016/0167-9457\(95\)00023-6](https://doi.org/10.1016/0167-9457(95)00023-6)
- Xu, T., Sheng, X., Zhang, T., Liu, H., Liang, X., & Ding, A. (2018). Development and validation of dummies and human models used in crash test. *Applied Bionics and Biomechanics*, *2018*. <https://doi.org/10.1155/2018/3832850>
- Yang, K. H., Hu, J., White, N. A., King, A. I., Chou, C. C., & Prasad, P. (2006). Development of Numerical Models for Injury Biomechanics Research: A Review of 50 Years of Publications in the Stapp Car Crash Conference. *SAE Technical Papers*, *2006-Novem*(November), 429–490. <https://doi.org/10.4271/2006-22-0017>
- Ye, X., Jones, D., Gaewsky, J., Miller, L., Stitzel, J., & Weaver, A. (2018). Numerical Analysis of Driver Thoracolumbar Spine Response in Frontal Crash Reconstruction. *Ohio State University Injury Biomechanics Symposium*, 1–14.
- Yoganandan, N., Mykiebust, J. B., Cusick, J. F., Wilson, C. R., & Sances, A. (1988). Functional biomechanics of the thoracolumbar vertebral cortex. *Clinical Biomechanics*, *3*(1). [https://doi.org/10.1016/0268-0033\(88\)90119-2](https://doi.org/10.1016/0268-0033(88)90119-2)
- Yoganandan, N., Pintar, F., Sances, A., Maiman, D., Myklebust, J., Harris, G., & Ray, G. (1988). Biomechanical investigations of the human thoracolumbar spine. *SAE Technical Papers*, *97*, 676–684. <https://doi.org/10.4271/881331>

Zador, P. L., & Ciccone, M. A. (1993). Automobile driver fatalities in frontal impacts: Air bags compared with manual belts. *American Journal of Public Health, 83*(5), 661–666. <https://doi.org/10.2105/AJPH.83.5.661>

APPENDIX

Table 1: Function, muscle layer classification, origin, insertion, PCSA, length and activation level curve used of each trunk muscle element implemented in this study

Muscle group	Muscle name	Number of elements	Function (Osth, 2010; Kenhub, n.d.)	Layer (Kenhub, n.d.)	Origin (Osth, 2010; GHBM HBM)	Insertion (Osth, 2010; GHBM HBM)	PCSA (mm ²) (Osth, 2010; Bogduk et al., 1992)	Length (mm)	Activation level curves used
Lumbar muscles	Multifidus thoracis	8	Lumbar extensor	Deep	Spinous process of T8 Spinous process of T9 Spinous process of T10 Spinous process of T10 Spinous process of T11 Spinous process of T11 Spinous process of T12 Spinous process of T12	Transverse process of L1 Transverse process of L1 Transverse process of L1 Transverse process of L2 Transverse process of L2 Transverse process of L3 Transverse process of L3 Transverse process of L4	25.0 45.0 39.0 65.0 29.0 90.0 53.0 118.0	127.6 108.3 90.4 118.5 91.3 126.7 105.6 134.3	Erector spinae

Muscle group	Muscle name	Number of elements	Function (Osth, 2010; Kenhub, n.d.)	Layer (Kenhub, n.d.)	Origin (Osth, 2010; GHBM HBM)	Insertion (Osth, 2010; GHBM HBM)	PCSA (mm ²) (Osth, 2010; Bogduk et al., 1992)	Length (mm)	Activation level curves used
	Multifidus lumborum	13	Lumbar extensor	Deep	Spinous process of L1 Spinous process of L1 Spinous process of L1 Spinous process of L1 Spinous process of L2 Spinous process of L2 Spinous process of L2 Spinous process of L3 Spinous process of L3 Spinous process of L4 Spinous process of L4 Spinous process of L5 Spinous process of L5	Mamillary process of L4 Mamillary process of L5 Sacrum Iliac crest Mamillary process of L5 Sacrum Iliac crest Sacrum Iliac crest Sacrum Iliac crest Sacrum Iliac crest	40.0 42.0 36.0 60.0 39.0 39.0 90.0 54.0 157.0 93.0 93.0 45.0 45.0	96.8 131.9 176.6 149.7 124.4 172.1 148.7 103.6 84.0 74.8 63.2 45.1 53.2	Erector spinae

Muscle group	Muscle name	Number of elements	Function (Osth, 2010; Kenhub, n.d.)	Layer (Kenhub, n.d.)	Origin (Osth, 2010; GHBM HBM)	Insertion (Osth, 2010; GHBM HBM)	PCSA (mm ²) (Osth, 2010; Bogduk et al., 1992)	Length (mm)	Activation level curves used
	Erector spinae Longissimus thoracis pars thoracis	12	Lumbar extensor	Superficial	7th rib 8th rib 8th rib 9th rib 9th rib 9th rib 10th rib 11th rib 11th rib 11th rib 11th rib 12th rib	Spinous process of L2 Spinous process of L2 Spinous process of L3 Spinous process of L4 Spinous process of L4 Spinous process of L5 Sacrum Sacrum Sacrum Sacrum Sacrum Sacrum	29.0 57.0 56.0 45.0 44.0 64.0 78.0 125.0 146.0 160.0 167.0 138.0	226.7 201.1 233.0 234.8 234.8 268.4 293.3 263.6 263.1 262.4 262.0 213.1	Erector spinae
	Erector spinae Longissimus thoracis pars lumborum	5	Lumbar extensor	Superficial	Transverse process of L1 Transverse process of L2 Transverse process of L3 Transverse process of L4 Transverse process of L5	Iliac crest Iliac crest Iliac crest Iliac crest Iliac crest	79.0 91.0 103.0 110.0 116.0	146.0 118.6 85.8 63.8 42.7	Erector spinae

Muscle group	Muscle name	Number of elements	Function (Osth, 2010; Kenhub, n.d.)	Layer (Kenhub, n.d.)	Origin (Osth, 2010; GHBM HBM)	Insertion (Osth, 2010; GHBM HBM)	PCSA (mm ²) (Osth, 2010; Bogduk et al., 1992)	Length (mm)	Activation level curves used
	Erector spinae Iliocostalis lumborum pars thoracis	8	Lumbar extensor	Superficial	12th rib 12th rib 12th rib 12th rib 12th rib 12th rib 12th rib 12th rib	Iliac crest Iliac crest Iliac crest Iliac crest Iliac crest Iliac crest Iliac crest Iliac crest	23.0 31.0 39.0 34.0 50.0 100.0 123.0 147.0	126.2 129.8 132.8 136.4 139.9 143.6 147.3 150.9	Erector spinae
	Erector spinae Iliocostalis lumborum pars lumborum	4	Lumbar extensor	Superficial	Transverse process of L1 Transverse process of L2 Transverse process of L3 Transverse process of L4	Iliac crest Iliac crest Iliac crest Iliac crest	108.0 154.0 182.0 189.0	140.2 112.8 82.7 62.6	Erector Spinae
Abdominal muscles	External oblique	2	Lumbar flexor	Superficial	Costal cartilage Costal cartilage	Iliac crest Iliac crest	452.4 452.4	125.0 104.9	External oblique
	Rectus abdominis	3	Lumbar flexor	Superficial	5th costal cartilage 6th costal cartilage 7th costal cartilage	Crest of pubis Crest of pubis Crest of pubis	189.0 189.0 189.0	304.8 288.8 278.8	Rectus abdominis

Muscle group	Muscle name	Number of elements	Function (Osth, 2010; Kenhub, n.d.)	Layer (Kenhub, n.d.)	Origin (Osth, 2010; GHBM HBM)	Insertion (Osth, 2010; GHBM HBM)	PCSA (mm ²) (Osth, 2010; Bogduk et al., 1992)	Length (mm)	Activation level curves used
	Quadratus lumborum	5	Lumbar flexor	Deep	12th rib Transverse process of L1 Transverse process of L2 Transverse process of L3 Transverse process of L4	Iliac crest Iliac crest Iliac crest Iliac crest Iliac crest	80.0 80.0 40.0 40.0 40.0	122.0 121.4 91.2 58.5 39.5	External oblique
	Internal oblique	2	Lumbar flexor	Deep	Costal cartilage Costal cartilage	Iliac crest Iliac crest	354.9 354.9	81.7 104.9	External oblique
Lower extremities muscle	Psoas major	6	Lumbar flexor	Deep	Vertebral body of T12 Vertebral body of L1 Vertebral body of L2 Vertebral body of L3 Vertebral body of L4 Vertebral body of L5	Femur head Femur head Femur head Femur head Femur head Femur head	241.5 241.5 262.0 364.0 239.0 115.0	350.7 322.9 293.2 262.7 229.1 204.3	External oblique

Note: lumbar extensors are usually considered as deep-layer muscles, therefore, relatively superficial lumbar extensors were classified as superficial muscles in this study